Received: 8 August 2022 | Revised: 17 January 2023 | Accepted: 31 January 2023

DOI: 10.1111/bph.16051

RESEARCH ARTICLE

Angiotensin deficient FVB/N mice are normotensive

André Felipe Rodrigues[1,2,3] | Mihail Todiras[1,4] | Fatimunnisa Qadri[1] | Natalia Alenina[1,3] | Michael Bader[1,3,5,6]

[1]Max-Delbrück-Center for Molecular Medicine in the Helmholtz Association, Berlin, Germany

[2]Department of Biology, Chemistry and Pharmacy, Free University of Berlin, Berlin, Germany

[3]German Center for Cardiovascular Research (DZHK), Partner Site Berlin, Berlin, Germany

[4]Nicolae Testemițanu State University of Medicine and Pharmacy, Chisinau, Moldova

[5]Charité Universitätsmedizin Berlin, Berlin, Germany

[6]Institute for Biology, University of Lübeck, Lübeck, Germany

Correspondence
Michael Bader, Max Delbrück Center for Molecular Medicine in the Helmholtz Association, Robert-Rössle-Str. 10, 13125 Berlin, Germany.
Email: mbader@mdc-berlin.de

Funding information
This work was supported by a grant of the German Research Foundation (Deutsche Forschungsgemeinschaft SFB1365) to N. A. and M. B.

Background and Purpose: All previous rodent models lacking the peptide hormone angiotensin II (Ang II) were hypotensive. A mixed background strain with global deletion of the angiotensinogen gene was backcrossed to the FVB/N background (Agt-KO), a strain preferred for transgenic generation. Surprisingly, the resulting line turned out to be normotensive. Therefore, this study aimed to understand the unique blood pressure regulation of FVB/N mice without angiotensin peptides.

Experimental Approach: Acute and chronic recordings of blood pressure (BP) in freely-moving adult mice were performed to establish baseline BP. The pressure responses to sympatholytic and sympathomimetic as well as a nitric oxide inhibitor and donor compounds were used to quantify the neurogenic tone and endothelial function. The role of the renal nerves on baseline BP maintenance was tested by renal denervation. Finally, further phenotyping was done by gene expression analysis, histology and measurement of metabolites in plasma, urine and tissues.

Key Results: Baseline BP in adult FVB/N Agt-KO was unexpectedly unaltered. As compensatory mechanisms Agt-KO presented an increased sympathetic nerve activity and reduced endothelial nitric oxide production. However, FVB/N Agt-KO exhibited the renal morphological and physiological alterations previously found in mice lacking the production of Ang II including polyuria and hydronephrosis. The hypotensive effect of bilateral renal denervation was blunted in Agt-KO compared to wild-type FVB/N mice.

Conclusion and Implications: We describe a germline Agt-KO line that challenges all previous knowledge on BP regulation in mice with deletion of the classical RAS. This line may represent a model of drug-resistant hypertension because it lacks hypotension.

KEYWORDS
angiotensin II, blood pressure, gene knockout, RAS

Abbreviations: 6-OHDA, 6-hydroxydopamine; Agt, angiotensinogen; RAS, renin angiotensin system; SNA, sympathetic nerve activity.

1 | INTRODUCTION

The classical renin angiotensin system (RAS or RAAS, renin angiotensin aldosterone system) committing the production of the peptide hormone **angiotensin II (Ang II)** in the circulation is a pivotal system controlling cardiovascular homeostasis as well as salt and water balance. Among the mechanisms by which Ang II regulates blood pressure (BP) are vascular smooth muscle contraction, aldosterone production and secretion, cardiac contractility, **vasopressin** release and sympathetic nerve activity (SNA). These physiological processes are in their majority mediated by the binding of Ang II to the **angiotensin type 1 receptor (AT_1)** expressed by different cell types in cardiovascular organs (Bader, 2010; Bekassy et al., 2022; Sequeira-Lopez & Gomez, 2021). The broad modulatory effects of Ang II on BP render **angiotensin-converting enzyme (ACE)** inhibitors and AT_1 antagonists (inhibiting Ang II/AT_1 axis) to be one of the most successful drug-based therapies to lower BP in human hypertension (Carey & Whelton, 2018). Humans have one gene encoding the AT_1 receptor, whereas rodents have two (*Agtr1a* and *Agtr1b*; AT_{1a} and AT_{1b}, respectively). Selective targeted deletion of these genes demonstrated that the AT_{1a} receptor is the major protein controlling cardiovascular homeostasis, because mice lacking the AT_{1a} receptor are hypotensive contrary to AT_{1b} deficient mice (Sparks et al., 2014).

All genes encoding proteins required for Ang II formation (the precursor protein angiotensinogen [Agt] and the two enzymes, **renin** and ACE) have been previously deleted in mouse models. All three mouse lines displayed hypotension, polyuria, polydipsia and post-natal renal morphological alterations including hydronephrosis (Krege et al., 1995; Takahashi et al., 2005; Tanimoto et al., 1994). These alterations were similar in double knockout mice lacking both AT_1 receptor subtypes demonstrating a fundamental role of the Ang II/AT_1 axis on BP control and renal development (Gembardt et al., 2008; Tsuchida et al., 1998).

Here, we present a puzzling finding considering all the knowledge acquired during the last three decades in animal model with gene targeted deletion of RAS proteins leading to the elimination of the Ang II/AT_{1a} axis in rodents. Surprisingly, FVB/N mice completely lacking Agt (Agt-KO) are normotensive. Comprehensive phenotyping of this line indicated that Agt-KO develop a strong neurogenic pressor activity compensating for the RAS loss.

What is already known

- Rodents lacking components of the angiotensin II/AT_{1a} axis are life-long hypotensive.

What does this study add

- The loss of the renin-angiotensin system in FVB/N mice has no effect on baseline blood pressure.
- Increased vascular tone due to exaggerated vascular sympathetic activity and reduced nitric oxide production prevent the blood pressure fall.

What is the clinical significance

- The unusual blood pressure regulation of FVB/N mice with depleted RAS may represent manifestations of human drug-resistant hypertension.

2 | METHODS

The Agt-KO mouse model (B6;CBAB6-*Agt*^{tm1Afu}, RRID:MGI:3699327) was previously generated as described by Tanimoto et al. (Tanimoto et al., 1994). The line was a gift from Prof. Dr. Akiyoshi Fukamizu. Originally, Agt-KO mice were obtained in a mixed background strain and the line was backcrossed for more than 10 generations with the FVB/N (FVB/NCrl; Charles Rivers #207, RRID:IMSR_CRL:207) strain at the animal facility of the Max Delbrück Center, Berlin. The FVB/N background strain is ideal for transgene mouse generation due to the large pronucleus that facilitates the microinjection of DNA constructs (Popova et al., 2005). Our group has generated and backcrossed several mouse lines to the FVB/N background strain to study the role of the RAS in cardiovascular control (Cardoso et al., 2010; Rodrigues et al., 2021; Rosendahl et al., 2014; Xu et al., 2008). Interestingly, by studying components of the protective arm of the RAS, our group has previously detected differences in cardiovascular control among FVB/N and C57BL/6 strains (Rabelo et al., 2016). Therefore, we decided to generate a RAS-deficient FVB/N line by means of genetically deleting the RAS precursor protein Agt.

2.1 | Animal experiments

All experiments involving animals (mice) are reported in compliance with the ARRIVE guidelines (Percie du Sert et al., 2020) as well as recommendations of the *British Journal of Pharmacology* (Lilley et al., 2020). Mice were kept in individually ventilated cages at a maximum number of 6 in a room with controlled temperature of 22 ± 1°C, under a standard light/dark cycle of 12 h each. All mice received commercial standard mouse chow and water *ad libitum*. For experiments, mice were transferred to experimental rooms at least 5 days prior to the experiment and were kept in conventional open cages covered with a polyester filter sheet. Food, water, room temperature and light schedule were kept as described above. All experiments were performed with adult male mice at 12 to 15 weeks of age. Surgical procedures were performed under anaesthesia with **ketamine** and **xylazine** (100 and 10 mg·Kg^{-1} *i.p.*, respectively) and **isoflurane** inhalation (1%–2%).

TABLE 1 List of vasoactive substances used in this study.

Substance	Manufacturer	Company reference
Angiotensin II acetate salt (Ang II)	Bachem	05-23-0101
Candesartan (CV 11974)	Tocris	4791/10
Dexmedetomidine hydrochloride	Tocris	2749
Endothelin-1 (ET-1)	Tocris	1160
Hexamethonium bromide	Sigma-Aldrich	H0879
Nifedipine	Tocris	1075
Nω-Nitro-L-arginine methyl ester hydrochloride (L-NAME)	Sigma-Aldrich	N5751
Phenylephrine	Sigma-Aldrich	P1250000
Prazosin hydrochloride	Tocris	0623
Sodium nitroprusside dihydrate (SNP)	Sigma-Aldrich	71,778
Tyramine	Sigma-Aldrich	T90344
Y27632 dihydrochloride	Tocris	1254
Yohimbine hydrochloride	Sigma-Aldrich	Y3125

Note: All drugs were diluted in sterile saline except for candesartan and nifedipine for which sterile saline was supplied with Na_2CO_3 (0,01%, w/v) and DMSO (5%, v/v), respectively.

During surgeries mice breath spontaneously and body temperature was maintained performing the procedure on a thermo-controlled plate that is connected to a rectal temperature sensor. Pain was managed providing 200 $mg \cdot kg^{-1} \cdot day^{-1}$ **metamizole** in drinking water before and after the surgeries. After any surgical procedure, mice were individually monitored at least once a day. *In vivo* experiments were performed at the animal facility of the Max Delbrück Center for Molecular Medicine, Berlin, following the EU directive 2010/63/EU for animal experiments. All *in vivo* procedures were previously approved by the Berlin State Office for Health and Social Affairs (Landesamt für Gesundheit und Soziales).

2.2 | Cardiovascular phenotyping

Acute BP recording with **heparin***-filled catheter:* Baseline acute BP and heart rate (HR) were recorded in freely moving mice using self-made catheters as previously described (Rodrigues et al., 2021; Todiras et al., 2017). Briefly, femoral catheters were implanted in the femoral artery and vein to reach the abdominal aorta and vena cava before the renal bifurcations. The catheters were exteriorized in the interscapular region and fixed with a silk-suture (3/0). Recordings of BP and HR were initiated 2 days after surgery in freely moving mice. Cardiovascular parameters were recorded constantly (beat-by-beat) at 200 Hz connecting the arterial catheter to a pressure transducer (AD Instruments #MLT0699) connected to a PowerLab/4sp via bridge amplifiers (AD Instruments #ML110). Baseline mean arterial pressure (MAP) and HR were obtained before any drug administration averaging the recorded data for ~1 h after a habituation period of the approximate same length. MAP was automatically calculated with the formula MAP = ((systolic + [2 x diastolic])/3) and the cardiac frequency (HR) was deduced from the oscillatory pressure waveform. The vascular response to several drugs was investigated *in vivo* using intravenous *bolus* injection of the substances and calculating the MAP response (Table 1). The acute maximal pressor or depressor responses to vasoactive drugs (ΔMAP) were calculated by the differences between the maximal MAP (peak or trough) response and the averaged MAP ~1 min before drug infusion (Todiras et al., 2017). Data analysis was carried out using the LabChart v5 software (AD Instruments). For quantifying the baroreflex control of HR, the ΔHR was calculated from doses of **phenylephrine** (1–10 $\mu g \cdot kg^{-1}$, i.v.) that triggered equi-pressor (~20 mmHg) MAP changes. The data is reported as the baroreflex sensitivity index calculated by the formula (BRS = ΔPI/ΔMAP, $ms \cdot mmHg^{-1}$). HR values where previously converted to pulse interval (PI, ms; 60,000/HR),and ΔPI = (peak response PI − baseline PI). All acute recordings of cardiovascular parameters and drug-induced pressure alterations were performed between ZT3 and ZT7.

Chronic BP recording with radiotelemetry: Telemetry probes (PhysioTel #PA-C10; DSI) were used to chronically record BP, HR and locomotor activity. The catheter of the pressure transmitter was inserted into the abdominal aorta via the femoral artery and the body of the transmitter was allocated in a subcutaneous pouch on the back of the mouse. Data acquisition started 12–14 days after surgery and data was recorded 24 h for 10 s every 5 min. Data were analysed with the software Dataquest ART.

2.3 | Cardiovascular response to chemical peripheral sympathetic ablation

Unspecific peripheral sympathectomy was used to assess the effect of sympathetic ablation on baseline cardiovascular parameters. After the establishment of the baseline cardiovascular parameters for 5 days mice received 6-hydroxydopamine hydrobromide (6-OHDA), a drug that destroys sympathetic terminals but does not penetrate the blood–brain barrier in adult rodents (Clark et al., 1972). 6-OHDA solutions were daily prepared in sterile physiological saline supplied with 0.01% **ascorbic acid**. Mice received five daily injections of 100 $mg \cdot kg^{-1}$ 6-OHDA i.p. Cardiovascular parameters were constantly recorded by radiotelemetry for 15 days (5 days before, 5 days during and 5 days after the 6-OHDA treatment).

2.4 | Renal denervation

Mice were previously instrumented with radiotelemetry probes as described above, but for this particular experiment the recording of baseline parameters was started 12–16 h after surgery. After baseline cardiovascular parameters recording for 48 h the animals underwent a total (afferent and efferent) renal denervation protocol. Renal denervation was performed exposing kidney and renal vessels by flank incisions (skin and muscle layers) under recovery anaesthesia. The kidney was gently retracted and all nerves visualized under a stereo

microscope were mechanically destroyed using fine surgical tools. To assure complete renal denervation, renal vessels were painted (~5 min) with a phenol solution (10% phenol in 95% ethanol). To prevent phenol spreading into the abdominal cavity parafilm was placed underneath the vessels and the excess of phenol was cleared with sterile physiological saline and cotton. Muscle and skin layers were closed separately with discontinuous sutures (silk 4/0) and the procedure repeated on the contralateral side. Animals recovered overnight (~12–16 h) in their home cage placed on a warm plate at 37°C. Post-denervation cardiovascular recordings were started immediately after recovery and lasted 1 week. The renal denervation success was evaluated by quantification of noradrenaline in each denervated kidney after 1 week as described below.

2.5 | Sample (organs, blood and urine) collection

Sampling was performed between ZT4 and ZT6 (4–6 after the onset of the light). The sample collection was done within these time points to match with the time that the acute cardiovascular phenotyping was undertaken.

Timed spontaneous urine was collected by holding the mouse over an empty tube. The procedure was repeated on the following 2 days in case additional urine was desired. After sampling, urine was snap frozen in dry ice and stored at −80°C until use.

Mice were killed by inhalation of an isoflurane overdose and blood was obtained using a 23G needle coupled to a 1-ml syringe from a cardiac puncture. EDTA-Plasma for western blot was prepared by collecting blood into MiniCollect® EDTA-K3 (Greiner #450531) coated tubes and centrifugation at 2000*g* for 10 min at 4°C. Plasma used for biochemical quantification of metabolites was performed as described above but collecting the blood into lithium-heparin coated tubes (Greiner #450537). Plasma samples were stored at −80°C until usage.

Kidneys used for histological analyses were collected into a 15 ml tube filled with buffered 4% paraformaldehyde and kept at room temperature until processing. Kidneys and liver used for molecular biology or biochemical measurements were harvested, shortly rinsed in ice cold PBS buffer (pH 7.4), transferred to a sterile tube and snap frozen in dry-ice. Thoracic aorta and mesenteric arteries were collected into a tube containing RNAlater solution (Sigma #R0901) and stored at 4°C for a maximum of 7 days. Fat and connective tissue were cleared from aorta and second/third branch mesenteric arteries placed under a stereomicroscope with fine surgical tools.

2.6 | Gene expression analyses

RNA extraction and cDNA synthesis: The trizol/chloroform method was used to extract RNA from kidney, liver, aorta and mesenteric arteries. Tissues were homogenized in 1 ml of Trizol (Invitrogen #15596018) using a FastPrep homogenization system with dedicated tubes and ceramic beads (MPI #116004500). To assure complete genomic DNA clearance, 1–5 µg of RNA was incubated with DNase I (Sigma, #04716728001). A cDNA library was generated from 0.5–2.0 µg of DNase I treated RNA, using M-MLV reverse transcriptase (Promega #M170B) following manufacturer's instructions.

Quantification of mRNA expression: Quantitative reverse transcription PCR (RT-qPCR) was performed using a SYBR green reagent mix following manufacturer's instructions. For these experiments, cDNA was diluted to a final concentration of 1 ng·µl^{-1} in nuclease-free water. RT-qPCRs were run in duplicates using a QuantStudio™ 5 device (Thermo Fischer #A28140). The acquired data was analysed using the software QuantStudio™ Design & Analysis Software v1.3.1 (Applied Biosystems). The Ct values obtained in the exponential phase of amplification from the gene of interest and an appropriate housekeeping gene (*Gapdh*, *Actb* or *18s*) were used to calculate the relative gene expression to the control group using the method of Livak and Schmittgen (Livak & Schmittgen, 2001) ($2^{-\Delta\Delta CT}$). A list of all specific primer pairs used for RT-qPCR is displayed in Table 2.

2.7 | Western blot

Immuno-related procedures used comply with the recommendations made by the *British Journal of Pharmacology* (Alexander et al., 2018). The absence of Agt protein in Agt-KO was verified using western blots with liver and plasma protein. Livers were homogenized in radioimmunoprecipitation assay (RIPA) buffer (100 mg·ml^{-1}, cell signalling #9806) supplemented with protease and phosphatase inhibitor cocktails using a benchtop homogenizer, FastPrep-24 (MP Biomedical #6004500). Samples were frozen and thawed three times, and centrifuged at 13.000 *g* for 10 min at 4°C. Finally, the supernatant was transferred to an empty tube. EDTA-plasma was diluted (1:10, v/v) in distilled water. Total proteins of liver extracts and diluted plasma were quantified using the bicinchoninic acid assay with a commercial kit (Sigma #BCA1-1KT). Samples were mixed with a 4X concentrated reducing buffer that is based on the Laemmli original formulation (Carl Roth #K929.1) and heated at 95°C for 5 min. Proteins were separated by molecular weight using 10% sodium dodecyl sulphate (SDS) polyacrylamide gels by electrophoresis. After electrophoresis proteins were transferred from the SDS gels to nitrocellulose membranes using a Trans-Blot Turbo (Bio-Rad #1704150). Afterwards membranes were blocked by incubation for 1 h at room temperature in a commercial blocking solution (Intercept, LI-COR #927-70001). After blocking membranes were incubated overnight at 4°C with a primary anti Agt antibody (1:100; IBL #28101, RRID:AB_2341481) diluted in an equal mixture of block solution and PBS-T (PBS plus 0.2% Tween-20). On the next day, membranes were washed in PBS-T and incubated with an anti-rabbit IRDye-800CW-conjugated secondary antibody diluted in PBS-T (green, 1:10,000; LI-COR #926-32213, RRID:AB_621848). Membranes were washed with PBS twice and scanned using an Odyssey infrared imaging system (LI-COR). The signals were visualized using the Image Studio Lite Software (LI-COR). The primary antibody procedure was repeated in the membrane containing liver protein extract by incubating the same membrane with a primary anti glyceraldehyde-3-phosphate dehydrogenase (GAPDH) antibody

TABLE 2 List of primer pairs used for RT-qPCR.

Target, *gene*	Sequence (5′ to 3′)	Sense	Amplicon size (bp)
18s, *Rn18s*	TTGATTAAGTCCCTGCCCTTTGT CGATCCGAGGGCCTCACTA	Forward Reverse	75
Agt, *Agt*	CTGAATGAGGCAGGAAGTGGG GCAGTCTCCCTCCTTCACAG	Forward Reverse	150
Aquaporin-2, *Aqp2*	ATGTGGGAACTCCGGTCCATA ACGGCAATCTGGAGCACAG	Forward Reverse	137
CD3, *CD3e*	ATGCGGTGGAACACTTTCTGG GCACGTCAACTCTACACTGGT	Forward Reverse	126
CD68, *Cd68*	TGTCTGATCTTGCTAGGACCG GAGAGTAACGGCCTTTTTGTGA	Forward Reverse	75
Collagen I, *Col1a1*	CTTCACCTACAGCACCCTTGTG GATGACTGTCTTGCCCCAAGTT	Forward Reverse	67
Collagen III, *Col3a1*	GCTGGCATTCCTCAGACTTCT ACTGTTTTTGCAGTGGTATGTAATG	Forward Reverse	67
Collagen IV, *Col4a1*	TCCGGGAGAGATTGGTTTCC CTGGCCTATAAGCCCTGGT	Forward Reverse	118
ENaCα, *Scnn1a*	CCAAGGGTGTAGAGTTCTGTGA AGAAGGCAGCCTGCAGTTTA	Forward Reverse	78
eNOS, *Nos3*	CCTTCCGCTACCAGCCAGA CAGAGATCTTCACTGCATTGGCTA	Forward Reverse	105
Fibronectin, *Fn1*	ACCATTACTGGTCTGGAGCC GGGTAACCAGTTGGGGAAGC	Forward Reverse	124
Gapdh, *Gapdh*	TCACCACCATGGAGAAGGC GCTAAGCAGTTGGTGGTGC	Forward Reverse	168
Icam, *Icam1*	TTCACACTGAATGCCAGCTC GTCTGCTGAGACCCCTCTTG	Forward Reverse	182
NCC, *Slc12a3*	ACACGGCAGCACCTTATACAT GAGGAATGAATGCAGGTCAGC	Forward Reverse	142
NHE3, *Slc9a3*	CAAGGTCACCAGTATCGTCCC GCATGAAGTATCCAGCATCCAAC	Forward Reverse	167
NKCC2, *Slc12a1*	GATGGGTGAAAGGTGTGCTG CAATTCCCGCTTCTCCTACAAT	Forward Reverse	96
PAX8, *Pax8*	ATGCCTCACAACTCGATCAGA ATGCGTTGACGTACAACTTCT	Forward Reverse	101
CCL5, *Ccl5*	GCTGCTTTGCCTACCTCTCC TCGAGTGACAAACACGACTGC	Forward Reverse	104
Renin, *Ren1* and *Ren2*	CAAAGTCATCTTTGACACGGG AGTCAGAGGACTCATAGAGGC	Forward Reverse	107
TGF-β, *Tgfb1*	CTTTGTACAACAGCACCCGC TAGATGGCGTTGTTGCGGTC	Forward Reverse	127
TNFα, *Tnf*	ACCCTCACACTCAGATCATCTTC TGGTGGTTTGCTACGACGT	Forward Reverse	71
Vcam, *Vcam1*	TGAACCCAAACAGAGGCAGAGT GGTATCCCATCACTTGAGCAGG	Forward Reverse	138
α_{1A} - *Adra1a*	CCAGCACAGGTGAACATTTC GATGCCGATGACAGGCCAC	Forward Reverse	118
$\alpha 1_{B}$ - *Adra1b*	ACATTGGGGTGCGATACTCTC TTGGGCGCAGGTTCTTTCC	Forward Reverse	139
α_{1D}- *Adra1d*	CGGACCTTCTGCGACGTATG TGGCTGGATACTTGAGCGAGT	Forward Reverse	124
α_{2A} - *Adra2a*	GGTGACACTGACGCTGGTTT ACTGGTGAACACCGCGATAATA	Forward Reverse	91

(Continues)

TABLE 2 (Continued)

Target, *gene*	Sequence (5′ to 3′)	Sense	Amplicon size (bp)
α_{2B} - *Adra2b*	GAGTCCAAGAAGCCCCATCC GGTGTCCATTAGCCTCTCCG	Forward Reverse	103
α_{2c} - *Adra2c*	TCTGGATCGGCTACTGCAAC GCTTGAAAGAGCGCCTGAAG	Forward Reverse	81
β-actin, *Actb*	CTGGCCTCACTGTCCACCTT CGGACTCATCGTACTCCTGCTT	Forward Reverse	61

(1:2000, Cell Signaling #2118, RRID:AB_561053) as described above. To distinguish the bands by colour an anti-rabbit IRDye-680RD-conjugated secondary antibody (red, 1:10000 LI-COR #926-68073, RRID:AB_10954442) was used.

2.8 | Plasma angiotensin II quantification

The absence of Ang II (angiotensin II) was verified in plasma of Agt-KO using a radioimmunoassay assay as previously described (Schelling et al., 1980).

2.9 | Noradrenaline quantification

Noradrenaline levels were measured using a commercial enzyme-linked immunosorbent assays (ELISA) kit following manufacturer's instructions (LDN #BA E-6200). Urine samples were readily used in the ELISA and tissues were homogenized in an extraction solution (0.01 N hydrochloric acid, 1-mM EDTA, 4-mM sodium disulfite) using a benchtop homogenizer, FastPrep-24 (MP Biomedical #6004500). Kidneys and mesenteric arteries were homogenized 1:40 and 1:100 (w/v), respectively.

2.10 | Total nitrates and nitrites quantification

The overall nitric oxide (NO) production was estimated by quantifying the products of NO metabolism (nitrates and nitrites) in timed urine. Urine samples were diluted 1:40 (v/v) in ultrapure water, nitrate was enzymatically converted to nitrite, and nitrite levels were quantified in urine with a commercial colorimetric assay kit following manufacturer's instructions (Cayman #780001). Nitrates and nitrites concentration was calculated using a nitrite standard curve and the concentration normalized by the urinary creatinine concentration.

2.11 | Plasma and urine clinical biochemistry

Timed urine and lithium-heparin plasma were used for this purpose. All measurements were performed by trained personnel at the animal phenotyping facility of the Max Delbrück Center for Molecular Medicine, Berlin, using an automated chemistry analyser (Beckman Coulter #AU480). The following parameters were measured in urine: sodium, potassium, albumin and creatinine, and plasma: sodium, potassium, chloride, albumin, total proteins, urea, creatinine, glucose. Blood urea nitrogen (BUN) was calculated using the formula BUN = (Urea*0.467). The relative urine volume between the two lines was calculated using inverse proportion of the creatinine concentration in the urine.

2.12 | Picrosirius red staining

Kidneys and hearts previously fixed in 4% buffered paraformaldehyde were dehydrated using ascending ethanol concentrations, embedded in paraffin, sectioned in 5-µm coronal sections using a rotary microtome (Thermo Fisher Scientific # HM 355S), mounted on SuperFrost Plus slides (Thermo Fisher Scientific) and stored at room temperature until staining. Before staining, organ sections were deparaffinized and rehydrated in xylol and descending ethanol concentrations. Renal and cardiac (left ventricular) fibrosis was stained with Picrosirius Red solution (0.1% Sirius red F3B in saturated aqueous solution of picric acid) for 1 h at room temperature. Finishing the incubation, the slides were washed twice with acidified tap water (0.5% glacial acetic acid), dehydrated (3X 100% ethanol), cleared using xylene and coverslipped using Eukitt (ORSAtec GmbH, Bobingen, Germany). Slides were allowed to air-dry for at least 24 h before light microscopy observation and pictures were taken using an inverted microscope (Keyence, #BZ-9000). Vascular and interstitial fibrotic areas were calculated using the BZ-II Analyzer software (Keyence, Osaka, Japan).

2.13 | Cardiomyocyte width

Deparaffinized and rehydrated mid-ventricular 3-µm heart sections were incubated with wheat germ agglutinin Alexa Fluor™ 488 Conjugate (1:500, Thermo Fisher Scientific #W11261) for 2 h at 37°C in wet chamber, washed three times with PBS for 10 min each and cover slipped using Vectashield antifade mounting medium containing DAPI (Vector Labo ratories #H-1200-10). Heart sections were visualized using an inverted microscope (Keyence, #BZ-9000) and

cardiomyocyte diameter measured using the using BZ-II Analyzer software (Keyence, Osaka, Japan).

2.14 | Data and statistical analyses

Experimental design as well as data and statistical analyses were performed in agreement with the guidelines of the British Journal of Pharmacology (Curtis et al., 2022). For all experiments randomization was applied and blinding whenever possible. The number of biological replicates is represented in the bar graphs by scatter plot whenever possible or indicated in the figure. To calculate the minimum number of replicates (equal number per group) to achieve statistical power, power analysis was applied using the software G Power 3.1. As parameters for power analysis, type I error was assumed at a significancy level of 0.05 and power of 80%. The main parameter for power analysis was the BP measurement by radiotelemetry. Data are presented as mean ± SD, including scattered plots in bar graphs and mean ± SE in repeated measure graphs. Two-tailed paired Student's *t* tests were used to test differences among two independent groups. To verify differences among two groups in which repeated measures were quantified, two-way ANOVA with repeated-measure tests were applied, and if F achieved $P < 0.05$ Dunnett's multiple comparison post hoc tests were used. Statistical analyses were only performed in groups containing at least five independent replicates (mice) using Graph Pad Prism. For all statistical tests used a $P < 0.05$ was considered statistically significant.

2.15 | Materials

Ketamine, xylazine, isoflurane and metamizole were purchased from CP Pharma #1202, #1205, #1214 and Ratiopharm #03530394, respectively. Trizol (guanidinium thiocyanate-phenol) was obtained from Invitrogen #15596026. Sodium dodecyl sulphate was purchased form Serva #20765.03. The following compounds were obtained from Sigma: 6-hydroxydopamine hydrobromide; 6-OHDA #162957, Chloroform 1.02445, EDTA #03609, ascorbic acid #A4544, and phenol #PHR1047. Compounds purchased from Carl Roth are the following: HCl #6792.1, ethanol #K928.4 and xylene #9713.3 and acrylamide/bis-acrylamide solution #A124.2. Details of other materials and suppliers are provided in the specific sections and table 1.l.

2.16 | Nomenclature of targets and ligands

Key protein targets and ligands in this article are hyperlinked to corresponding entries in the IUPHAR/BPS Guide to PHARMACOLOGY http://www.guidetopharmacology.org and are permanently archived in the Concise Guide to PHARMACOLOGY 2021/22 (Alexander et al., 2021).

3 | RESULTS

3.1 | Baseline cardiovascular homeostasis in FVB/N Agt-KO

Baseline cardiovascular parameters were initially established in freely moving Agt-KO using heparin-saline filled catheters implanted into the abdominal aorta via the femoral artery. Interestingly, Agt-KO backcrossed to the FVB/N inbred strain did not exhibit the expected reduced mean arterial pressure (MAP) by 20 mmHg or more as previously described in other mouse strains (Table S1). Figure 1a shows normal baseline MAP levels in Agt-KO (110 ± 8.0 mmHg versus 107.1 ± 2.8 mmHg in wildtype). Moreover, baseline heart rate (HR) was not different between Agt-KO and FVB/N controls (Figure 1a). To ascertain these findings, we chronically monitored BP using radiotelemetry. Consistently, FVB/N Agt-KO presented normal baseline MAP (106.4 ± 4.3 mmHg vs. 102.0 ± 4.4 mmHg in controls) and unaltered HR (Figure 1c) confirming the findings of the acute recordings. Additionally, locomotor activity was equal between Agt-KO and controls (Figure 1c). Further telemetric measurements revealed that systolic pressure and pulse pressure were even increased in Agt-KO but diastolic pressure was not different from controls (Figure 1c). Finally, heart weight and cardiomyocyte width, parameters that normally vary according to baseline BP levels, were found increased in Agt-KO (Figure 1b). Additionally, heart sections containing the left ventricle were stained with picrosirius red for fibrosis quantification (Figure S3a). Figure S3c shows that Agt-KO present increased interstitial left ventricle collagen accumulation. Body weight as well as kidney, lungs, spleen and adrenal glands wet weights were not different among adult FVB/N wildtype and Agt-KO (Table S2).

For the purpose of better visualization, the data recorded by radiotelemetry was hourly averaged and plotted (Figure 1d). Agt-KO presented a circadian rhythmicity in all measured parameters similar to wildtype mice. A differential (day and night) calculation of the cardiovascular parameters is displayed in the Figure S2. Curiously, MAP of Agt-KO was increased in the dark phase (active phase) and this effect was not paralleled by HR or locomotor activity changes discarding an involvement of both parameters in the BP circadian rhythm (Figures 1d and S2). Additionally, Agt-KO presented increased systolic pressure and pulse pressure especially during the dark phase (Figures 1c and S2b,d). The high nocturnal systolic pressure likely contributes to the increased nocturnal MAP levels found in Agt-KO (Figure S2a). Altogether, Agt-KO on the FVB/N background are normotensive during the day (resting phase) and even slightly hypertensive in the night (active phase).

To ascertain that Agt is not expressed in our backcrossed FVB/N Agt-KO line, RT-qPCRs and western blots were used. Quantification of *Agt* mRNA in liver samples of Agt-KO demonstrated absence of Agt expression (Figure S1a,b). Confirming this finding plasma and liver of Agt-KO mice lack immunoreactivity for the ~53 kDa Agt band present in controls (Figure S1c,d). In addition, we demonstrated the

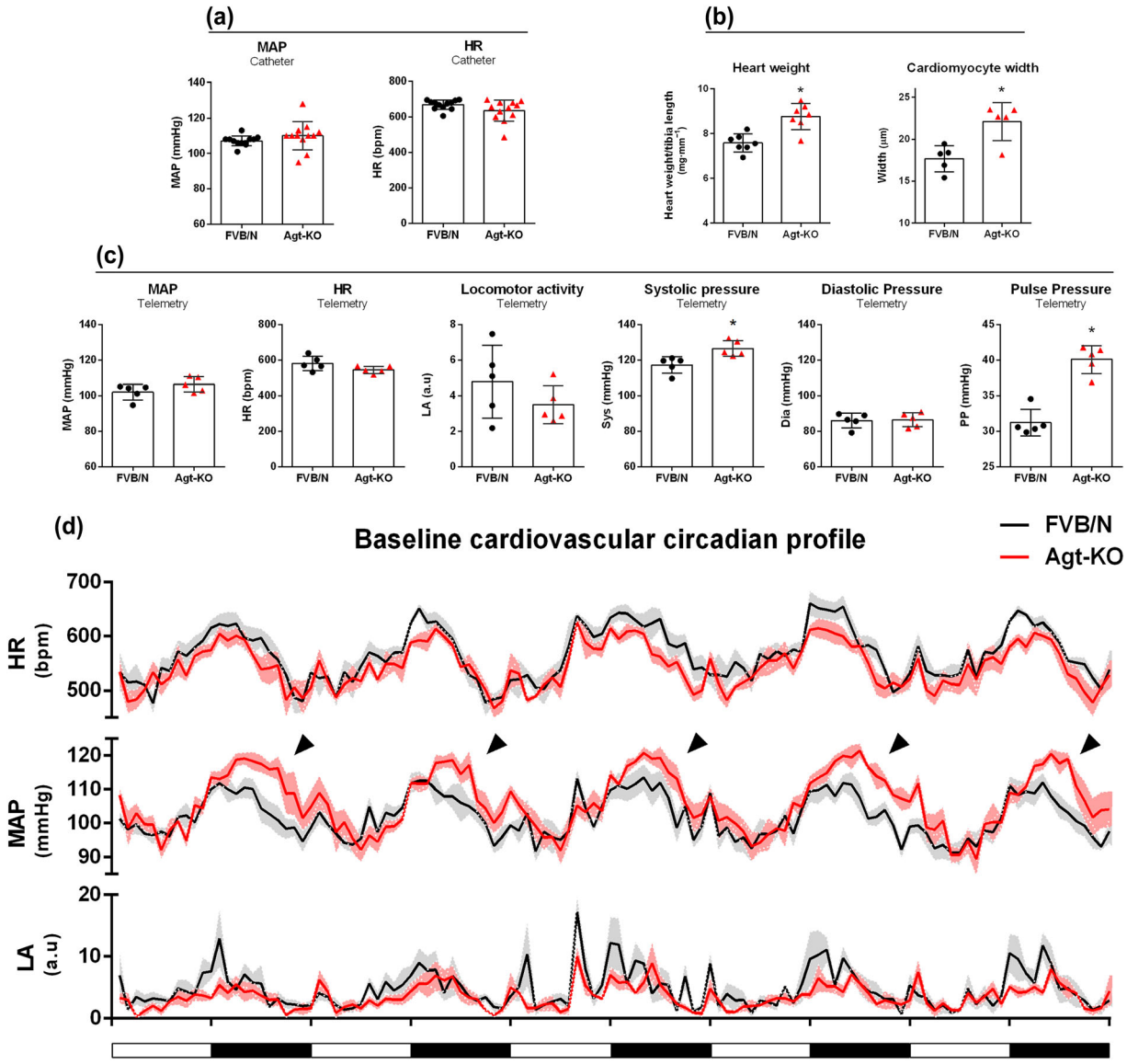

FIGURE 1 Baseline cardiovascular phenotyping of Agt-KO. (a) Short-term measurement of baseline MAP (left panel) and HR (right panel) using fluid-filled catheters in freely-moving mice. (b) Heart weight to tibia length ratio (left panel) and left ventricular cardiomyocyte width (right panel). (c) Long-term (5 days 24 h averaged) baseline cardiovascular parameters from left to right: MAP, HR, systolic pressure, diastolic pressure and pulse pressure as well as locomotion recorded by radiotelemetry. (d) Circadian profile of the HR, MAP and in FVB/N wildtype and Agt-KO obtained by continuous telemetry recordings for five consecutive days. Arrow heads are pointing to increased MAP values in the active phase. Filled and white intervals below the x axis represent dark and light periods, respectively. For (a)–(c) values are mean ± SD *P <0.05 versus FVB/N (Student's t test). For (d), values are the hour average for each parameter ± SEM for five animals in each group. MAP = mean arterial pressure; HR = heart rate; LA = locomotor activity; Sys = systolic; Dia = diastolic; PP = pulse pressure; a.u = arbitrary units.

presence of a functional response to Ang II in our FVB/N mice showing that the peptide triggered an increase in MAP similarly in wild-types and Agt-KO (Figure S1e). In agreement, a sub-chronic treatment with the AT_1 antagonist **candesartan** reduced MAP in control mice but not in Agt-KO (Figure S1F). These results combined demonstrated functional AT_1 receptors as well as the absence of Ang II. We further verified the lack of Ang II in plasma of Agt-KO by radioimmunoassay and thereby also excluded the existence of any other precursor protein for angiotensins (Figure S1g).

3.2 | Neurogenic pressor activity

We hypothesized that the sympathetic nervous system is hyperactive in Agt-KO to compensate for the lack of the RAS. To test this hypothesis, the mice used for cardiovascular phenotyping by radiotelemetry underwent a peripheral sympathectomy by administration of 6-hydroxydopamine (6-OHDA), whereas their cardiovascular parameters were recorded. In support of our hypothesis, Agt-KO presented a larger MAP response to 6-OHDA in comparison to controls indicating

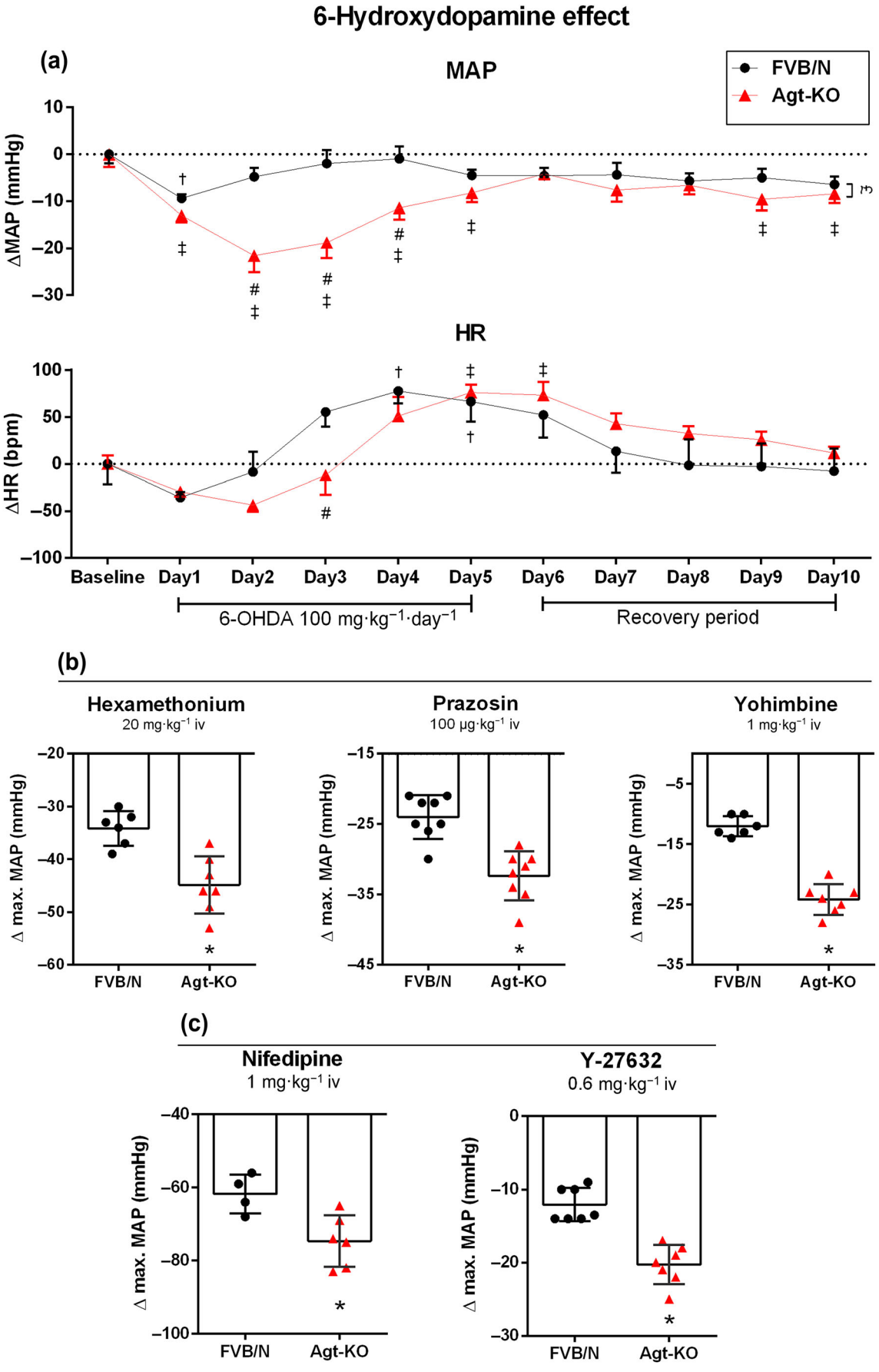

FIGURE 2 MAP response to chemical sympathectomy and sympatholytic drugs. (a) baseline change in MAP (ΔMAP, top panel) and HR (ΔHR, lower panel) to peripheral chemical sympathectomy performed by five daily consecutive injections (intraperitoneal) of 6-hydroxydopamine (6-OHDA). (b) Maximal MAP response induced by the ganglionic blocker hexamethonium (left panel) and to the α_1 antagonist prazosin (middle panel) or the α_2 antagonist yohimbine (right panel) in freely moving mice. (c) Maximal MAP response to the L-type calcium channel blocker nifedipine (left panel) and the ROCK kinases inhibitor Y27632 (right panel) in freely moving mice (c). For (a) values are mean ± SEM for five animals in each group $^{\#}P < 0.05$ versus FVB/N at the same time point. $^{\dagger}P < 0.05$ post-sympathectomy versus FVB/N baseline. $^{\ddagger}P < 0.05$, Agt-KO post-sympathectomy versus Agt-KO baseline; $^{£}P < 0.05$, Agt-KO versus FVB/N post-sympathectomy; (two-way ANOVA with repeated measurements followed by Bonferroni's multiple comparison post hoc test). For (b) and (c) values are mean ± SD $^{*}P < 0.05$ versus FVB/N (Student's *t* test). MAP = mean arterial pressure; HR = heart rate; i.v. = intravenous.

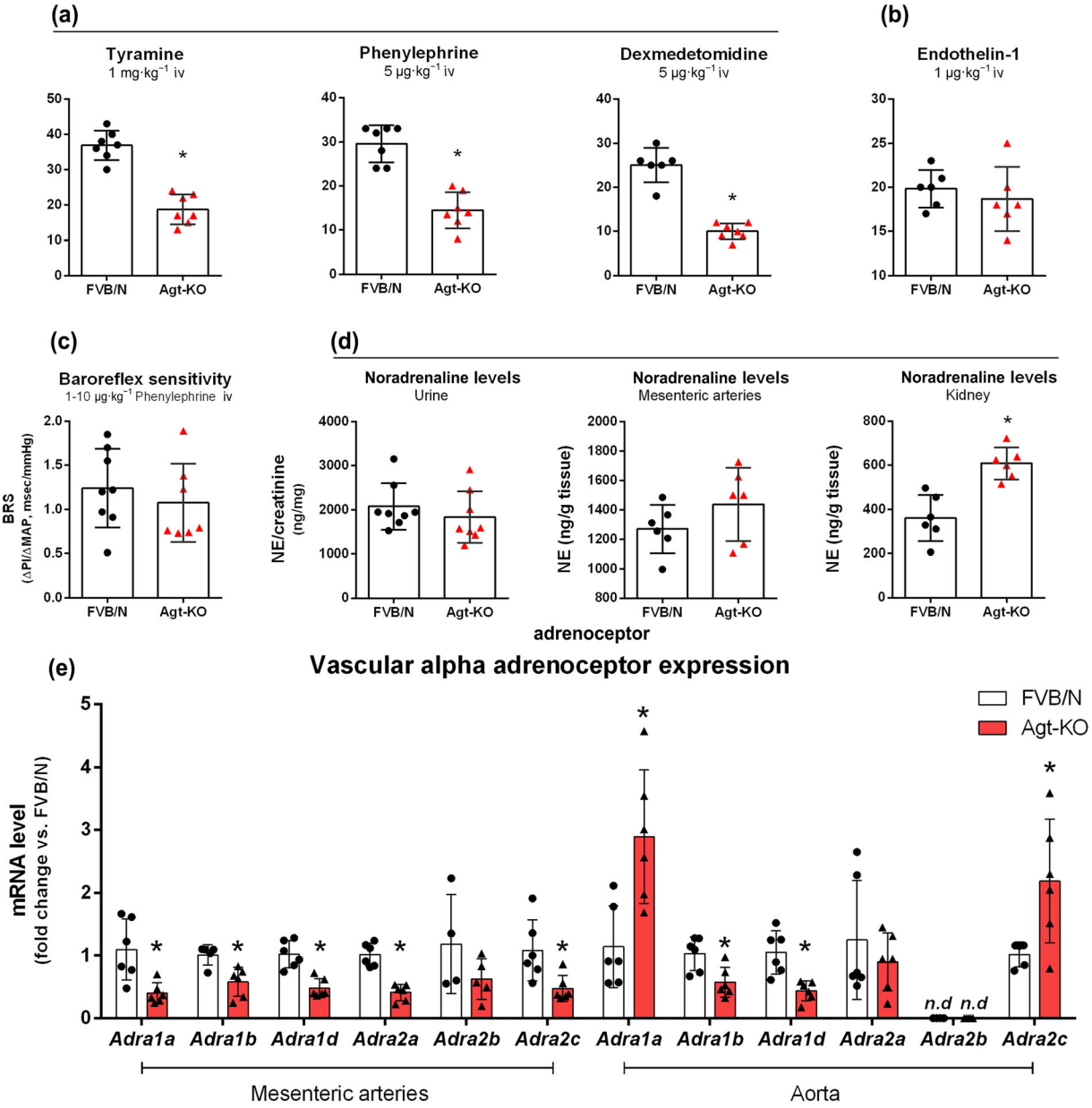

FIGURE 3 MAP response to sympathomimetic drugs, baroreflex sensitivity of the HR and tissue noradrenaline (NE) measurements. (a) Maximal MAP response elicited by sympathomimetic drugs in freely-moving mice: - tyramine (releases endogenous NE, left panel), phenylephrine (α_1 agonist, middle panel) and dexmedetomidine (α_2 agonist, right panel). (b) Maximal MAP response to endothelin-1 (ET-1) in freely moving mice. (c) Baroreflex sensitivity of the HR calculated from equi-pressor doses of phenylephrine, ~20 mmHg, in freely moving mice. (d) Quantification of NE in urine (left panel), mesenteric arteries (middle panel) and kidneys (right panel). (e) Quantification of mRNA levels of α-adrenoceptors in mesenteric arteries and aorta. α_{1A} = *Adra1a*; α_{1B} = *Adra1b*; α_{1D} = *Adra1d*; α_{2A} = *Adra2a*; α_{2B} = *Adra2b*; α_{2C} = *Adra2c*. Values are mean ± SD $^{*}P < 0.05$ versus FVB/N (Student's *t* test). MAP = mean arterial pressure; HR = heart rate; i.v. = intravenous; BRS = baroreflex sensitivity.

a stronger BP dependence on sympathetic nerve activity (SNA). Interestingly, MAP recovered to levels close to baseline even before the end of the 6-OHDA treatment in both controls and Agt-KO (Figure 2a). After the cessation of the 6-OHDA treatment, BP and vascular sympathetic innervation are known to be restored in rats. Moreover, other mechanisms as augmented vascular adrenergic reactivity and adrenal catecholamine production as well as activation of the RAS were previously described in sympathectomized rats (Finch et al., 1973; Obayashi et al., 2000; Porlier et al., 1977; Vavřínová et al., 2019). 6-OHDA causes a long-term generalized peripheral sympathetic ablation. Therefore, the immediate MAP response to intravenously injected sympatholytic drugs was quantified to estimate the influence of the SNA on the vascular tone. Agt-KO presented a stronger MAP response in mice treated with the ganglion blocker **hexamethonium** as well as those treated with either the α_1 and α_2 **adrenoceptor** antagonists **prazosin** and **yohimbine**, respectively (Figure 2b).

Because the vascular tone is influenced by a myriad of vasoactive substances that could potentially buffer the neurogenic tone, unselective blockers targeting calcium dependent and calcium independent pathways of the vascular constrictor machinery were used. **Nifedipine**, a L-type channel calcium blocker and **Y27632**, a ROCK kinase inhibitor, were injected intravenously and the maximal depressor effect on MAP quantified. Agt-KO displayed stronger MAP responses to both drugs indicating an increased basal vascular tone (Figure 2c).

Peripheral endogenous noradrenaline was released using **tyramine** to test if the increased response to sympatholytic drugs is mediated by increased vascular reactivity to noradrenaline. Interestingly, Agt-KO presented a reduced pressor response to tyramine (Figure 3a). To ascertain that this phenotype is not due to reduced vesicular noradrenaline content, the MAP responses to controlled concentrations of α adrenoceptor agonists (α_1, phenylephrine and α_2, **dexmedetomidine**) were investigated. The pressor responses to these sympathomimetic compounds were also blunted in Agt-KO (Figure 3a). However, infusion of **endothelin-1** (ET-1) led to a similar pressor response indicating that vascular constriction is not impaired (Figure 3b) and analyses of the baroreflex control of the HR showed also no alterations in Agt-KO (Figure 3c and Table S3). RT-qPCRs were used for quantifying the expression of α adrenoceptors in thoracic aorta and mesenteric arteries. Interestingly, the gene expression of the most relevant α adrenoceptors controlling vascular smooth muscle contraction were down-regulated in Agt-KO (Figure 3f). Finally, noradrenaline was quantified in mesenteric arteries and urine by ELISA and found to be unaltered in Agt-KO (Figure 3d).

3.3 | Endothelial function

Endothelial-derived nitric oxide (NO) is a major factor counteracting vasoconstriction. NO homeostasis was assessed *in vivo* using the changes in MAP triggered upon the administration of the NO synthase blocker **L-NAME** and the NO donor **sodium nitroprusside**. Agt-KO presented a decreased MAP response to L-NAME (Figure 4a) and increased response to sodium nitroprusside (Figure 4b), indicating an impaired production of NO. The mRNA of **endothelial NO synthase** (eNOS) was quantified by RT-qPCR and Agt-KO exhibited reduced gene expression of this enzyme in aorta (Figure 4c) and mesenteric arteries (Figure 4d). Finally, the end-products of NO metabolism nitrate and nitrites were found reduced in the urine of Agt-KO (Figure 4e) confirming the *in vivo* findings.

3.4 | Renal damage and function

Mice with global deletion of the RAS components (Agt, renin and angiotensin converting enzyme) develop a typical renal morphology marked by atrophy of the renal papilla, hydronephrosis, fibrosis and concentric vascular hypertrophy of the renal arterial tree (Ding et al., 2001; Kihara, 1998). FVB/N Agt-KO also presented these common alterations in kidney sections (Figure 5a). Picrosirius-red staining revealed peritubular, perivascular, periglomerular and intra-arterial collagen accumulation in Agt-KO (Figure 5a–c). Collagen **COL1A1** and **COL3A1** mRNA expression was likewise increased in Agt-KO but **COL4A1** expression was not altered (Figure 5d). Accordingly, the mRNA levels of **fibronectin**, an essential protein for fibrillogenesis, were found increased in Agt-KO (Figure 5d). Interestingly, the expression of **transforming growth factor beta (TGF-β)**, a master regulator of collagen secretion and fibroblast differentiation, was only slightly up-regulated in Agt-KO (Figure 5d). In addition, kidneys of Agt-KO presented increased infiltration of leucocytes measured by mRNA quantification of CD68 and **CD3**, which are macrophage- and T-cell-specific markers, respectively (Figure S4a,b). The mRNA levels of the proinflammatory cytokines **TNF-α** and **CCL5** were increased in Agt-KO kidneys (Figure S4c,d). The finding of increased leucocytes in Agt-KO kidneys is supported by increased expression of **vascular cell adhesion protein-1 (VCAM-1)** and **intercellular adhesion molecule-1 (ICAM-1)**, which are essential mediators for leucocyte infiltration (Figure S4e,f).

Renal renin expression is regulated by multiple control mechanisms such as BP, Ang II levels and SNA. Therefore, it was interesting to quantify renin gene expression by RT-qPCR. Strikingly, the normotensive FVB/N Agt-KO showed similar renin mRNA levels in comparison to controls (Figure 5d) despite the absence of Ang II (Figure S1g) and likely increased renal SNA, as estimated by measurements of kidney noradrenaline (Figure 3d).

Plasma urea and creatinine were increased in Agt-KO suggesting a reduced glomerular filtration rate (Table 3). Agt-KO presented increased plasma sodium (Table 3) as well as total protein and albumin concentrations indicating dehydration (Table 3). Moreover, urine concentration ability was impaired in FVB/N Agt-KO as described in previous reports on other Agt-deficient mouse strains (Kihara, 1998; Okubo et al., 1998) (~3X higher volume, Table 3). As consequence of a high urinary output, sodium and potassium concentrations were strongly diluted in the urine of Agt-KO (Table 3). Despite the morphological alterations, the renal damage marker albumin normalized by

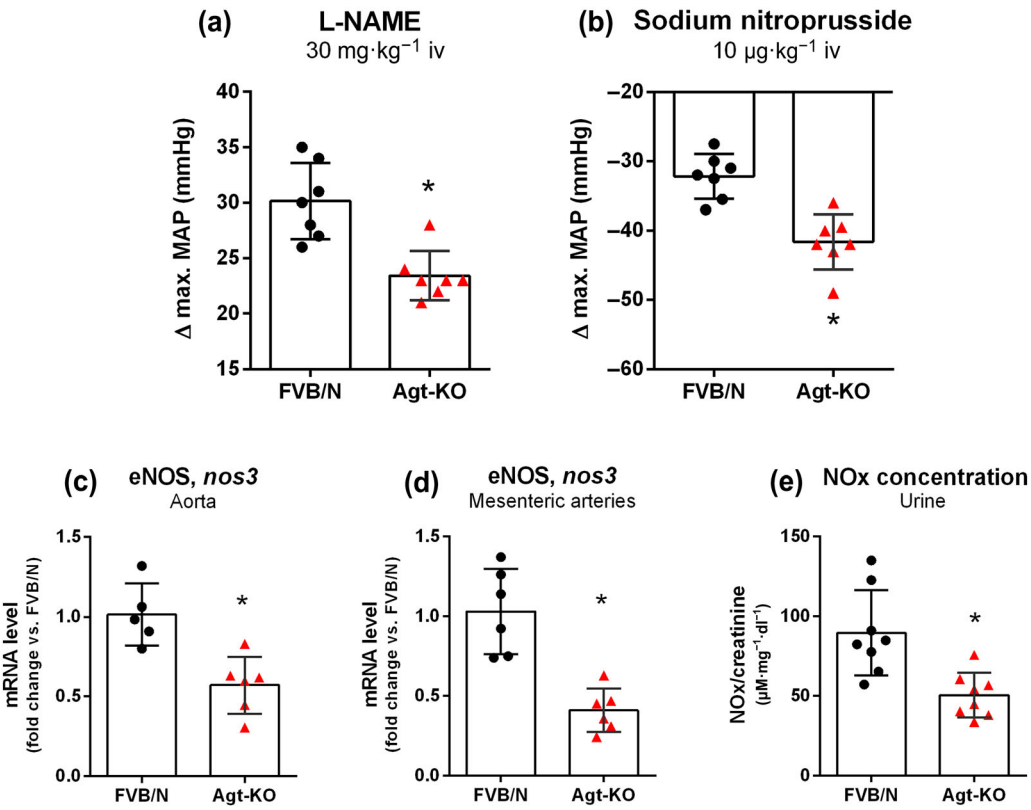

FIGURE 4 Vascular endothelial function. (a,b) Maximal MAP response induced by the NO synthase inhibitor N^G-*nitro-L-arginine methyl ester* (L-NAME) (a) and to the NO donor sodium nitroprusside (b) in freely moving mice. (c,d) mRNA expression of endothelial NO synthase (eNOS) in aorta (c) and mesenteric arteries (d). (e) Urinary total nitrate and nitrite (NOx) levels. Values are mean ± SD *$P < 0.05$ versus FVB/N (Student's *t* test). MAP = mean arterial pressure; i.v. = intravenous.

the creatinine concentration was only marginally increased in Agt-KO (Table 3).

Furthermore, we investigated renal gene expression of the most relevant renal tubular proteins involved in sodium reabsorption. The expression of the **sodium-hydrogen exchanger 3 (NHE3)** was not altered (Figure S5a). The mRNA levels of the genes encoding the **sodium-potassium-chloride (NKCC2)**, **sodium-chloride transporter (NCC)** and α-subunit of **epithelial sodium transporter (ENaC)** were down-regulated in Agt-KO (Figure S5b–d). Tubular cell number is apparently unaltered because expression of the epithelial cell marker Pax8 (Tong et al., 2009) was not different (Figure S5e). Finally, the mRNA levels of the water channel **aquaporin-2 (AQP2)** were quantified by RT-qPCR in kidney but no differences were detected (Figure S5f).

To verify if renal afferent and/or efferent nerve activity influence the baseline BP in Agt-KO, a bilateral total renal denervation was performed and the changes in MAP monitored. MAP was immediately reduced in wildtype mice by ∼15 mmHg after renal denervation and this effect was sustained over a week (Figures 6a and S6a). Interestingly, Agt-KO presented only a slight and gradual MAP reduction after denervation peaking around 4 to 5 days after surgery (Figures 6a and S6a). The HR increased the day after surgery in controls and Agt-KO, and gradually returned to baseline levels in controls, but it remained elevated (∼40 bpm) in Agt-KO for over a week (Figures 6b and S6b). Before renal denervation Agt-KOs were normotensive but their HR was reduced by ∼40 bpm (Figure S6a,b). The increased HR after denervation is not preventing MAP to fall in Agt-KO because it was not different between the lines during the first 2 days after denervation, whereas MAP in controls already markedly dropped. Possible mechanisms behind the renal denervation-induced tachycardia in Agt-KO are altered sympatho-vagal balance or dehydration caused by reduced renal urine concentrating ability. The success of the renal denervation procedure was verified by measuring ∼90% reduced renal noradrenaline at the end of the *in vivo* recordings (Figure S7). Altogether, the renal denervation revealed that the renal nerves and the increased renal SNA are not involved in the unexpectedly high levels of baseline BP in FVB/N Agt-KO. Moreover, it showed that the BP lowering effect of renal denervation in wildtype mice relies on an intact RAS.

4 | DISCUSSION

We have backcrossed a previously described hypotensive Agt-KO line (Tanimoto et al., 1994) to the FVB/N background and failed to measure the expected hypotension. Investigating the source of

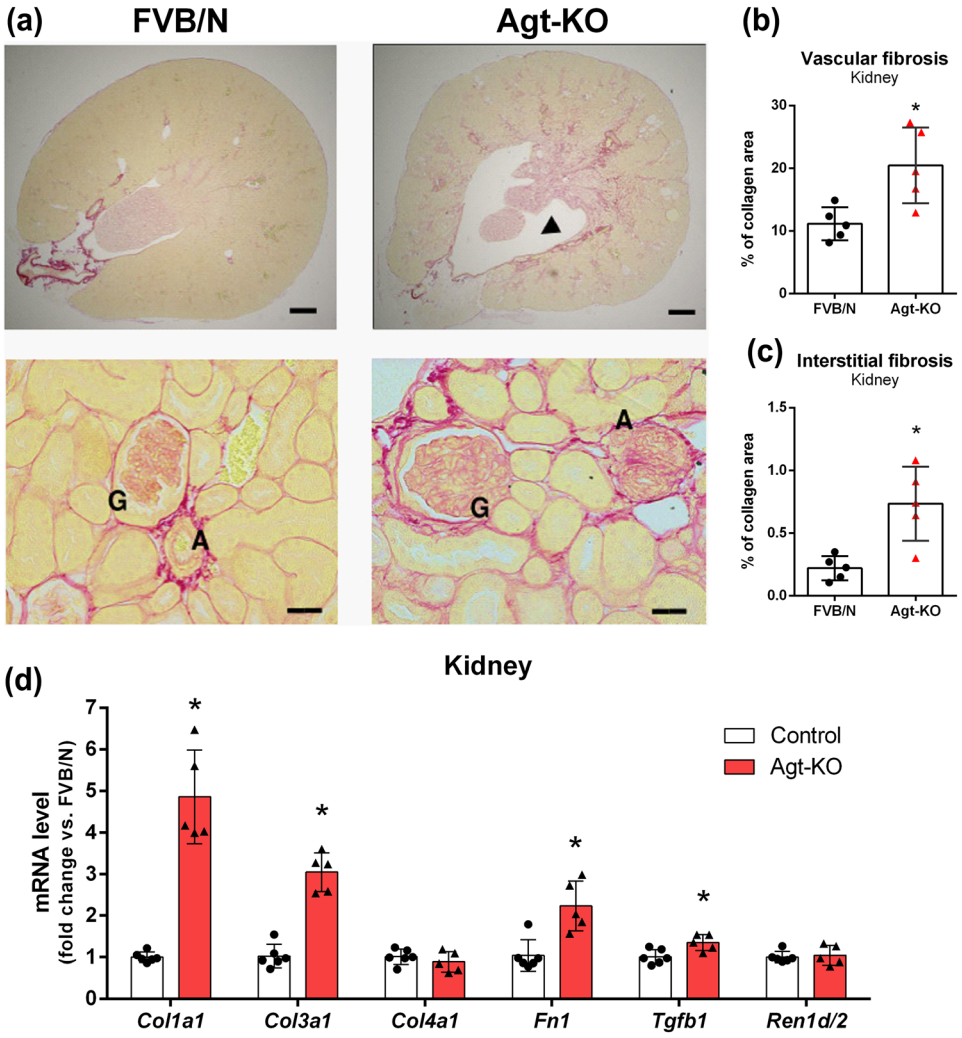

FIGURE 5 Renal morphology and renal expression of fibrosis markers and renin. (a) histochemical collagen staining with Picrosirius-red in representative kidney sections. Top panels are showing diffuse collagen accumulation (pink) in Agt-KO as well as reduced medullary area due to hydronephrosis and atrophy of the renal papilla. Lower panels are showing increased perivascular and intravascular fibrosis in Agt-KO. Arrowhead = hydronephrosis, G = glomerulus, A = artery. Top panels scale bars are 500 µm, lower panels bars are 40 µm. (b) Renal vascular (perivascular + intravascular) fibrotic area quantification. (c) Renal interstitial fibrotic area quantification. (d) Renal mRNA levels of collagen I (*Col1a1*), collagen III (*Col3a1*), collagen IV (*Col4a1*), fibronectin (*Fn1*), transforming growth factor beta (TGF-β, *Tgfb1*) and renin (*Ren1d and Ren2*). For (b)–(d) values are mean ± SD *$P < 0.05$ (Student's *t* test).

TABLE 3 Plasma and urine biochemical parameters.

Plasma			Urine		
Parameter (unit)	**FVB/N (n = 6)**	**Agt-KO (n = 6)**	**Parameter (unit)**	**FVB/N (n = 8)**	**Agt-KO (n = 8)**
CRE ($mg \cdot dl^{-1}$)	0.12 ± 0.01	0.17 ± 0.01*	Na^+ ($mmol \cdot L^{-1}$)	93.4 ± 39.8	28.6 ± 7.7*
BUN ($mg \cdot dl^{-1}$)	26.8 ± 2.3	81.4 ± 8.0*	K^+ ($mmol \cdot L^{-1}$)	242.7 ± 45.9	102.8 ± 14.9*
Na^+ ($mmol \cdot L^{-1}$)	147.6 ± 0.6	150.6 ± 2.2*	ALB ($\mu g \cdot dl^{-1}$)	608.8 ± 68.0	327.5 ± 174.2*
K^+ ($mmol \cdot L^{-1}$)	7.01 ± 0.66	7.40 ± 0.50	CRE ($mg \cdot dl^{-1}$)	30.9 ± 5.6	9.9 ± 0.9*
Cl^- ($\mu g \cdot dl^{-1}$)	107.1 ± 0.77	110.6 ± 2.77*	$[Na^+] \cdot [K^+]^{-1}$	0.39 ± 0.20	0.28 ± 0.08
$[Na^+] \cdot [K^+]^{-1}$	21.2 ± 2.1	20.3 ± 1.6	$[Na^+] \cdot [CRE]^{-1}$	2.99 ± 1.17	2.92 ± 0.83
TP ($g \cdot L^{-1}$)	50.0 ± 1.2	53.1 ± 2.3*	$[K^+] \cdot [CRE]^{-1}$	8.11 ± 2.28	10.40 ± 1.09*
ALB ($g \cdot L^{-1}$)	25.5 ± 1.4	27.8 ± 1.1*	$[ALB] \cdot [CRE]^{-1}$	20.2 ± 3.9	32.3 ± 15.2*
GLC ($mg \cdot dl^{-1}$)	271.3 ± 37.1	262.2 ± 53.7	eUvol. (% of FVB/N)	102.6 ± 17.5	314.8 ± 28.0*

Note: Values are displayed as mean ± SD. CRE = creatinine, BUN = blood urea nitrogen, Na^+ = sodium, K^+ = potassium, Cl^- = chloride, TP = total proteins, ALB = albumin, GLC = glucose, [ALB] = albumin concentration, [CRE] = creatinine concentration, $[K^+]$ = potassium concentration, $[Na^+]$ = sodium concentration, eUvol. = estimated urinary volume.
*$P < 0.05$ versus FVB/N (Student's *t* test).

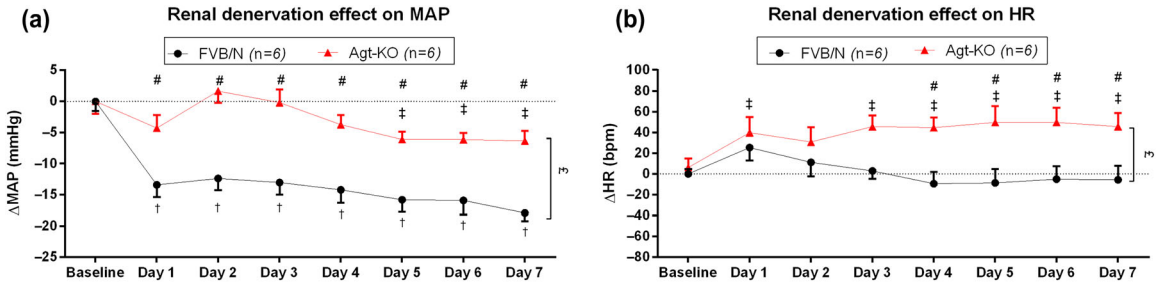

FIGURE 6 Effect of renal denervation on cardiovascular homeostasis. (a) Renal denervation effect on MAP. (b) Renal denervation effect on HR. Values are mean ± SE $^{\#}P < 0.05$ versus FVB/N at the same time point. $^{\dagger}P < 0.05$ FVB/N post-denervation versus FVB/N baseline. $^{\ddagger}P < 0.05$, Agt-KO post-denervation versus Agt-KO baseline; $^{£}P < 0.05$, Agt-KO versus FVB/N post-denervation; (two-way ANOVA with repeated measurements followed by Bonferroni's multiple comparison post hoc test). MAP = mean arterial pressure; HR = heart rate.

normotension led us to uncover increased sympathetic vasomotor tone and impaired endothelial NO production as compensatory mechanisms. Furthermore, renal morphology and function was similarly impaired in the FVB/N Agt-KO line as in all other animals lacking a functional RAS. Finally, renal denervation excluded a possible involvement of the renal nerves in the compensatory mechanism normalizing baseline BP in FVB/N Agt-KO.

The gene encoding the RAS precursor protein Agt has been successfully deleted in mice resulting in hypotension reported by at least 14 independent studies (Table S1) using mice of different background strains: Mixed background (129 × C57BL/6J, 129/Ola × C57BL/6, CBA × C57BL/6 or CBA × C57BL/6 × NMRI), C57BL/6, C57BL/6J, ICR and even in FVB/N. Furthermore, the genetic deletion of the enzymes of the Ang II formation pathway (renin [Takahashi et al., 2005; Yanai et al., 2000] and angiotensin-converting enzyme [Cole et al., 2000; Esther et al., 1996; Krege et al., 1995]) as well as the AT_{1a} (Ito et al., 1995; Sugaya et al., 1995) or both AT_{1a} and AT_{1b} double-knockout (Gembardt et al., 2008; Oliverio et al., 1998; Tsuchida et al., 1998) resulted in hypotension in mice. More recently, renin and AT_{1a} knockout rats were generated and reported as hypotensive (Exner et al., 2020; Moreno et al., 2011). The difference of baseline BP (systolic pressure or MAP) values between wildtypes and Agt-KOs varies from ∼15–50 mmHg across the different studies and the previously published FVB/N Agt-KO presented the smallest difference (14 mmHg). These studies used different methodologies and conditions to measure baseline BP (involving anaesthesia or not) and mice of different age and background strains, thus, differences are not surprising. We detected normotension in FVB/N Agt-KO employing two methodologies in freely-moving mice including radiotelemetry chronic recordings, which is the current gold standard to measure baseline BP in rodents (Carnevale et al., 2021; Kurtz et al., 2005). In contrast, the previously described slight hypotension in FVB/N Agt-KO was detected by tail-cuff plethysmography, which includes light anaesthesia and may therefore have moderated SNA (Lochard et al., 2003). Interestingly, one study already observed an effect of anaesthesia on baseline BP in Agt-KO: MAP in Agt-KO on a mixed genetic background differed from wildtypes by ∼35 and ∼50 mmHg in recordings performed in freely-moving and anaesthetised mice, respectively (Table S1) (Tsuchida et al., 1998).

Renin release and expression are largely controlled by baseline BP levels (Ehmke et al., 1987; Holmer et al., 1994; Watanabe et al., 2021). Consistently, hypotension in Agt-KO from previous studies caused marked increases in kidney renin mRNA (Ishida et al., 1998; Nakamori et al., 2018; Tamura et al., 1998; Tanimoto et al., 1994). In contrast, the normotensive Agt-KO presented unaltered kidney renin mRNA again confirming that the Ang II feedback on renin expressing cells is not a determinant of renal renin expression (Matsusaka et al., 1996; Neubauer et al., 2018). Furthermore, most RAS deleted mice had lighter hearts due to life-long hypotension (Gembardt et al., 2008; Kang et al., 2002; Tamura et al., 1998). Normotensive Agt-KO has an increased cardiac mass, which may reflect the increased active phase MAP and systolic pressure.

The neural control of the vascular tone is an important player in baseline BP control. Increased neurogenic tone is commonly found in association with primary hypertension and several models of hypertension and the mechanisms associated to BP increase are direct vascular constriction and vascular remodelling (Aalkjær et al., 2021; Asirvatham-Jeyaraj et al., 2021; DeLalio et al., 2020; Jama et al., 2022). The neurogenic pressor activity was not previously measured in Agt-KO using sympatholytic drugs, only plasma noradrenaline levels were measured but they were not altered (Sun et al., 2003). Another study found increased renal noradrenaline consistent to our findings in FVB/N Agt-KO (Nakamori et al., 2018). We found increased response to long-term and short-term sympatholytic drugs. However, acutely administered sympathomimetic agents exerted diminished responses. This phenotype was accompanied by decreased expression of the major α_1 and α_2 adrenoceptors in the vasculature. *In vitro* studies indicated that Ang II induces α-adrenoceptor expression in cultured rat smooth muscle cells (Hu et al., 1995; Lázaro-Suárez et al., 2011). Additionally, the reduced receptor expression might be a mechanism to mitigate increased SNA as observed during heart failure (Lohse et al., 2003). Taken together, the increased hypotensive response to generalized sympathectomy, different sympatholytic and unspecific vasorelaxants confirmed an exaggerated neurogenic tone in Agt-KO resulting in increased vasoconstriction powerfully preventing baseline BP to fall in the absence of Ang II.

On top of the increased neurogenic tone, the NO production was reduced in our Agt-KO line. Endothelial NO is essential to counteract

diverse vasoconstrictor stimuli by increasing smooth-muscle **cGMP** (Farah et al., 2018). Therefore, the reduced NO in Agt-KO likely contributes to sustain the normotensive baseline BP. Increased Ang II has been previously associated with impaired vascular NO synthesis and increased BP (Laursen et al., 1997; Rabelo et al., 2016). In agreement with that a previous study with severely hypotensive Agt-KO demonstrated increased NO metabolites in urine and plasma contrary to our findings (Sun et al., 2003). Altogether, changes in the neurogenic tone and endothelial NO production that resemble human primary hypertension are maintaining normal BP in FVB/N Agt-KO.

The lack of Ang II/AT_1 axis during nephrogenesis leads to postnatal renal morphological alterations in rodents with genetic deletion of RAS components (Hilgers et al., 1997; Ishida et al., 1998; Pentz et al., 2004; Sequeira-Lopez & Gomez, 2021; Takahashi et al., 2005) or treated with RAS blockers after birth (Deluque et al., 2020; Madsen et al., 2010). At birth the renal morphology of Agt-KO is comparable to controls, but in the first weeks of life alterations including papillary atrophy, hydronephrosis and vascular concentric hypertrophy develop (Nagata et al., 1996; Niimura et al., 1995; Tsuchida et al., 1998). In addition, fibrosis and infiltration of monocytes were previously demonstrated in Agt-KO and renin knockout mice in agreement with our findings (Kang et al., 2002; Nakamori et al., 2018; Niimura et al., 1995; Takahashi et al., 2005). Our study demonstrated that these alterations are BP independent but solely dependent on the lack of Ang II in early postnatal life. Increased plasma markers of renal and muscular function, urea and creatinine, suggest reduced glomerular filtration rate consistent with previous data from renin knockout mice (Takahashi et al., 2005). The same study reported no albuminuria corresponding to the minimal albuminuria found in our study. Interestingly, the gene expression of major tubular sodium transporters NKCC2, NCC and ENaC was decreased in kidneys of FVB/N Agt-KO despite a greater urinary volume. Hydronephrosis is likely the cause because a similar phenomenon was described in ureter ligation-induced experimental hydronephrosis (Li et al., 2003; Zhang et al., 2015).

Renal sympathetic efferents increases BP by distinct mechanisms involving renin expression/release, renal vascular resistance control and salt and water reabsorption (Osborn et al., 2021; Osborn & Foss, 2017). Additionally renal pathologies with increased immune cell infiltration and intrarenal pressure may activate the renal afferents and invert the reno-renal-reflex causing neurogenic hypertension (Banek et al., 2019; Lopes et al., 2020; Osborn et al., 2021). However, these mechanisms are not involved in the FVB/N Agt-KO normotension because renal denervation minimally reduced its baseline BP. In wildtype mice, BP decreased strongly and immediately after denervation compared to the small, slow and gradual reduction in Agt-KO, which is probably caused by increased natriuresis (Osborn & Foss, 2017). The strong BP reduction in FVB/N wildtype mice is compatible with previous observations in denervated wildtype Sprague–Dawley rats that supports a role of the renal nerves in baseline BP maintenance. Selective afferent renal denervation has no effect on baseline BP in these rats, thus, renal efferents control baseline BP (Banek et al., 2016; Foss et al., 2015; Jacob et al., 2003; Osborn & Foss, 2017). However, other studies denervated the same rat strain and found no baseline BP alterations, which is compatible to findings from other rat strains and mice (Asirvatham-Jeyaraj et al., 2016; Foss et al., 2018; Gueguen et al., 2019; Hohl et al., 2022; Moreira et al., 2020; Xiao et al., 2015). Further studies have to be performed to test if the species and/or background strain or rather technical issues like denervation efficacy are decisive. Because Agt-KO differ from wildtype FVB/N mice by the lack of the RAS precursor Agt, a possible mechanism behind the exclusive BP fall in wildtype mice after renal denervation is reduced renal renin production/release and consequently Ang II formation.

Altogether, we presented a completely unexpected BP phenotype in FVB/N mice with germline Agt deletion when compared to all previous studies with Agt-KO in the literature (Table S1). As compensatory mechanism for the lack of the RAS, FVB/N Agt-KO exhibit increased SNA to the vasculature accompanied by reduced NO production. The renal morphology and physiology are similar to what was previously described and the renal nerves are not contributing to the normotension in this line.

5 | LIMITATIONS AND FUTURE DIRECTIONS

Described below are limitations of this study that might be further addressed in follow up studies on the model. The data presented is essentially from young adult male mice, sex-and-age differences would be interesting to be evaluated, especially to further understand the BP regulation in FVB/N Agt-KO. Some conclusions drawn from this study rely on mRNA quantifications rather than direct protein quantifications, which might provide a more robust analysis. Urine volume was estimated by creatinine levels in timed spotted urine. The 24-h total urine collection would allow a more precise quantification of volume and metabolite/mineral output. Moreover, direct recordings of renal sympathetic nerves should be performed to provide a better evaluation of the actual nerve activity than noradrenaline measurements. The study shows reduced vascular eNOS expression with a vascular effect in Agt-KO. However, the mechanism downregulating eNOS is unknown and future studies may address whether also increased oxidative stress and eNOS uncoupling contributes to low NO generation in FVB/N Agt-KO. Finally, the FVB/N Agt-KO may have increased vascular stiffness because pulse pressure is increased. Pulse wave velocity analyses should be performed to confirm if these mice indeed present increased vascular stiffness.

DECLARATION OF TRANSPARENCY AND SCIENTIFIC RIGOUR

This Declaration acknowledges that this paper adheres to the principles for transparent reporting and scientific rigour of preclinical research as stated in the *BJP* guidelines for Design & Analysis, Immunoblotting and Immunochemistry and Animal Experimentation, and as recommended by funding agencies, publishers and other organizations engaged with supporting research.

AUTHOR CONTRIBUTIONS

The study was designed by A. R., M. T. and M. B. Data collection was performed by A. R., M. T., F. Q. and N. A., whereas data analysis was performed by A. R. The study was supervised by M. B. A. R. and M. B. drafted the manuscript. All authors reviewed and approved the final version of the manuscript.

ACKNOWLEDGEMENTS

We thank Prof. Dr. Roland Veelken for his expert advice on the renal denervation procedure. We are grateful for the technical assistance of Andrea Rodak and Ilona Kamer as well as for the clinical chemistry services of the Animal Phenotyping platform of the Max Delbrück Center, Berlin. Open access funding enabled and organized by Projekt DEAL.

CONFLICT OF INTEREST

None.

DATA AVAILABILITY STATEMENT

The data that support the findings of this study are available from the corresponding author upon reasonable request. Some data may not be made available because of privacy or ethical restrictions.

ORCID

André Felipe Rodrigues https://orcid.org/0000-0002-7219-6896

REFERENCES

Aalkjær, C., Nilsson, H., & De Mey, J. G. R. (2021). Sympathetic and sensory-motor nerves in peripheral small arteries. *Physiological Reviews*, *101*(2), 495–544. https://doi.org/10.1152/physrev.00007.2020

Alexander, S. P., Christopoulos, A., Davenport, A. P., Kelly, E., Mathie, A., Peters, J. A., Veale, E. L., Armstrong, J. F., Faccenda, E., Harding, S. D., Pawson, A. J., Southan, C., Davies, J. A., Abbracchio, M. P., Alexander, W., Al-hosaini, K., Bäck, M., Barnes, N. M., Bathgate, R., … Ye, R. D. (2021). THE CONCISE GUIDE TO PHARMACOLOGY 2021/22: G protein-coupled receptors. *British Journal of Pharmacology*, *178*(S1), S27–S156. https://doi.org/10.1111/bph.15538

Alexander, S. P. H., Roberts, R. E., Broughton, B. R. S., Sobey, C. G., George, C. H., Stanford, S. C., Cirino, G., Docherty, J. R., Giembycz, M. A., Hoyer, D., Insel, P. A., Izzo, A. A., Ji, Y., MacEwan, D. J., Mangum, J., Wonnacott, S., & Ahluwalia, A. (2018). Goals and practicalities of immunoblotting and immunohistochemistry: A guide for submission to the *British Journal of Pharmacology*. *British Journal of Pharmacology*, *175*, 407–411. https://doi.org/10.1111/bph.14112

Asirvatham-Jeyaraj, N., Fiege, J. K., Han, R., Foss, J., Banek, C. T., Burbach, B. J., Razzoli, M., Bartolomucci, A., Shimizu, Y., Panoskaltsis-Mortari, A., & Osborn, J. W. (2016). Renal denervation normalizes arterial pressure with no effect on glucose metabolism or renal inflammation in obese hypertensive mice. *Hypertension*, *68*(4), 929–936. https://doi.org/10.1161/HYPERTENSIONAHA.116.07993

Asirvatham-Jeyaraj, N., Gauthier, M. M., Banek, C. T., Ramesh, A., Garver, H., Fink, G. D., & Osborn, J. W. (2021). Renal denervation and celiac Ganglionectomy decrease mean arterial pressure similarly in genetically hypertensive Schlager (BPH/2J) mice. *Hypertension*, *77*(2), 519–528. https://doi.org/10.1161/HYPERTENSIONAHA.119.14069

Bader, M. (2010). Tissue renin-angiotensin-aldosterone systems: Targets for pharmacological therapy. *Annual Review of Pharmacology and Toxicology*, *50*(1), 439–465. https://doi.org/10.1146/annurev.pharmtox.010909.105610

Banek, C. T., Gauthier, M. M., Van Helden, D. A., Fink, G. D., & Osborn, J. W. (2019). Renal inflammation in DOCA-salt hypertension. *Hypertension*, *73*(5), 1079–1086. https://doi.org/10.1161/HYPERTENSIONAHA.119.12762

Banek, C. T., Knuepfer, M. M., Foss, J. D., Fiege, J. K., Asirvatham-Jeyaraj, N., Van Helden, D., Shimizu, Y., & Osborn, J. W. (2016). Resting afferent renal nerve discharge and renal inflammation. *Hypertension*, *68*(6), 1415–1423. https://doi.org/10.1161/HYPERTENSIONAHA.116.07850

Bekassy, Z., Lopatko Fagerström, I., Bader, M., & Karpman, D. (2022). Crosstalk between the renin–angiotensin, complement and kallikrein–kinin systems in inflammation. *Nature Reviews Immunology*, *22*(7), 411–428. https://doi.org/10.1038/s41577-021-00634-8

Cardoso, C. C., Alenina, N., Ferreira, A. J., Qadri, F., Lima, M. P., Gross, V., Todiras, M., Pesquero, J. B., Pesquero, J. L., & Bader, M. (2010). Increased blood pressure and water intake in transgenic mice expressing rat tonin in the brain. *Biological Chemistry*, *391*(4), 435–441. https://doi.org/10.1515/BC.2010.040

Carey, R. M., & Whelton, P. K. (2018). Prevention, detection, evaluation, and Management of High Blood Pressure in adults: Synopsis of the 2017 American College of Cardiology/American Heart Association hypertension guideline. *Annals of Internal Medicine*, *168*(5), 351–358. https://doi.org/10.7326/M17-3203

Carnevale, L., Carnevale, R., Mastroiacovo, F., Cifelli, G., Carnevale, D., & Lembo, G. (2021). Ultrasound-guided catheter implantation improves conscious radiotelemetric blood pressure measurement in mice. *Cardiovascular Research*, *117*(3), 661–662. https://doi.org/10.1093/cvr/cvab011

Clark, D. W., Laverty, R., & Phelan, E. L. (1972). Long-lasting peripheral and central effects of 6-hydroxydopamine in rats. *British Journal of Pharmacology*, *44*(2), 233–243. https://doi.org/10.1111/j.1476-5381.1972.tb07259.x

Cole, J., Ertoy, D., Lin, H., Sutliff, R. L., Ezan, E., Guyene, T. T., Capecchi, M., Corvol, P., & Bernstein, K. E. (2000). Lack of angiotensin II-facilitated erythropoiesis causes anemia in angiotensin-converting enzyme-deficient mice. *Journal of Clinical Investigation*, *106*(11), 1391–1398. https://doi.org/10.1172/JCI10557

Curtis, M. J., Alexander, S. P. H., Cirino, G., George, C. H., Kendall, D. A., Insel, P. A., Izzo, A. A., Ji, Y., Panettieri, R. A., Patel, H. H., Sobey, C. G., Stanford, S. C., Stanley, P., Stefanska, B., Stephens, G. J., Teixeira, M. M., Vergnolle, N., & Ahluwalia, A. (2022). Planning experiments: Updated guidance on experimental design and analysis and their reporting III. *British Journal of Pharmacology*, *179*, 3907–3913. https://doi.org/10.1111/bph.15868

DeLalio, L. J., Sved, A. F., & Stocker, S. D. (2020). Sympathetic nervous system contributions to hypertension: Updates and therapeutic relevance. *Canadian Journal of Cardiology*, *36*(5), 712–720. https://doi.org/10.1016/j.cjca.2020.03.003

Deluque, A. L., de Almeida, L. F., Francescato, H. D. C., da Silva, C. G. A., Costa, R. S., Antunes-Rodrigues, J., & Coimbra, T. M. (2020). Effect of calcitriol on the renal microvasculature differentiation disturbances induced by AT1 blockade during Nephrogenesis in rats. *Frontiers in Medicine*, *7*, 23. https://doi.org/10.3389/fmed.2020.00023

Ding, Y., Stec, D. E., & Sigmund, C. D. (2001). Genetic evidence that lethality in angiotensinogen-deficient mice is due to loss of systemic but not renal angiotensinogen. *Journal of Biological Chemistry*, *276*(10), 7431–7436. https://doi.org/10.1074/jbc.M003892200

Ehmke, H., Persson, P., & Kirchheim, H. (1987). Pressure-dependent renin release: The kidney factor in long-term control of arterial blood pressure in conscious dogs. *Clinical and Experimental Hypertension. Part a: Theory and Practice*, *9*(sup1), 181–195. https://doi.org/10.3109/10641968709160173

Esther, C. R., Howard, T. E., Marino, E. M., Goddard, J. M., Capecchi, M. R., & Bernstein, K. E. (1996). Mice lacking angiotensin-converting enzyme have low blood pressure, renal pathology, and reduced male fertility. *Laboratory Investigation*, *74*(5), 953–965. http://www.ncbi.nlm.nih.gov/pubmed/8642790

Exner, E. C., Geurts, A. M., Hoffmann, B. R., Casati, M., Stodola, T., Dsouza, N. R., Zimmermann, M., Lombard, J. H., & Greene, A. S. (2020). Interaction between Mas1 and AT1RA contributes to enhancement of skeletal muscle angiogenesis by angiotensin-(1-7) in dahl salt-sensitive rats. *PLoS ONE*, *15*(4), e0232067. https://doi.org/10.1371/journal.pone.0232067

Farah, C., Michel, L. Y. M., & Balligand, J.-L. (2018). Nitric oxide signalling in cardiovascular health and disease. *Nature Reviews Cardiology*, *15*(5), 292–316. https://doi.org/10.1038/nrcardio.2017.224

Finch, L., Haeusler, G., Kuhn, H., & Thoenen, H. (1973). Rapid recovery of vascular adrenergic nerves in the rat after chemical sympathectomy with 6-hydroxydopamine. *British Journal of Pharmacology*, *48*(1), 59–72. https://doi.org/10.1111/j.1476-5381.1973.tb08222.x

Foss, J. D., Fiege, J., Shimizu, Y., Collister, J. P., Mayerhofer, T., Wood, L., & Osborn, J. W. (2018). Role of afferent and efferent renal nerves in the development of AngII-salt hypertension in rats. *Physiological Reports*, *6*(3), e13602. https://doi.org/10.14814/phy2.13602

Foss, J. D., Wainford, R. D., Engeland, W. C., Fink, G. D., & Osborn, J. W. (2015). A novel method of selective ablation of afferent renal nerves by periaxonal application of capsaicin. *American Journal of Physiology-Regulatory, Integrative and Comparative Physiology*, *308*(2), R112–R122. https://doi.org/10.1152/ajpregu.00427.2014

Gembardt, F., Heringer-Walther, S., Esch, J. H. M., Sterner-Kock, A., Veghel, R., Le, T. H., Garrelds, I. M., Coffman, T. M., Danser, A. H. J., Schultheiss, H.-P., & Walther, T. (2008). Cardiovascular phenotype of mice lacking all three subtypes of angiotensin II receptors. *The FASEB Journal*, *22*(8), 3068–3077. https://doi.org/10.1096/fj.08-108316

Gueguen, C., Jackson, K. L., Marques, F. Z., Eikelis, N., Phillips, S., Stevenson, E. R., Charchar, F. J., Lambert, G. W., Davern, P. J., & Head, G. A. (2019). Renal nerves contribute to hypertension in Schlager BPH/2J mice. *Hypertension Research*, *42*(3), 306–318. https://doi.org/10.1038/s41440-018-0147-9

Hilgers, K. F., Reddi, V., Krege, J. H., Smithies, O., & Gomez, R. A. (1997). Aberrant renal vascular morphology and renin expression in mutant mice lacking angiotensin-converting enzyme. *Hypertension*, *29*(1 II), 216–221. https://doi.org/10.1161/01.HYP.29.1.216

Hohl, M., Selejan, S.-R., Wintrich, J., Lehnert, U., Speer, T., Schneider, C., Mauz, M., Markwirth, P., Wong, D. W. L., Boor, P., Kazakov, A., Mollenhauer, M., Linz, B., Klinkhammer, B. M., Hübner, U., Ukena, C., Moellmann, J., Lehrke, M., Wagenpfeil, S., … Böhm, M. (2022). Renal denervation prevents atrial Arrhythmogenic substrate development in CKD. *Circulation Research*, *130*(6), 814–828. https://doi.org/10.1161/CIRCRESAHA.121.320104

Holmer, S., Rinne, B., Eckardt, K. U., Le Hir, M., Schricker, K., Kaissling, B., Riegger, G., & Kurtz, A. (1994). Role of renal nerves for the expression of renin in adult rat kidney. *American Journal of Physiology-Renal Physiology*, *266*(5), F738–F745. https://doi.org/10.1152/ajprenal.1994.266.5.F738

Hu, Z. W., Shi, X. Y., Okazaki, M., & Hoffman, B. B. (1995). Angiotensin II induces transcription and expression of alpha 1-adrenergic receptors in vascular smooth muscle cells. *American Journal of Physiology-Heart and Circulatory Physiology*, *268*(3), H1006–H1014. https://doi.org/10.1152/ajpheart.1995.268.3.H1006

Ishida, J., Sugiyama, F., Tanimoto, K., Taniguchi, K., Syouji, M., Takimoto, E., Horiguchi, H., Murakami, K., Yagami, K.-I., & Fukamizu, A. (1998). Rescue of Angiotensinogen-Knockout Mice. *Biochemical and Biophysical Research Communications*, *252*(3), 610–616. https://doi.org/10.1006/bbrc.1998.9707

Ito, M., Oliverio, M. I., Mannon, P. J., Best, C. F., Maeda, N., Smithies, O., & Coffman, T. M. (1995). Regulation of blood pressure by the type 1A angiotensin II receptor gene. *Proceedings of the National Academy of Sciences*, *92*(8), 3521–3525. https://doi.org/10.1073/pnas.92.8.3521

Jacob, F., Ariza, P., & Osborn, J. W. (2003). Renal denervation chronically lowers arterial pressure independent of dietary sodium intake in normal rats. *American Journal of Physiology - Heart and Circulatory Physiology*, *284*(6 53–6), 2302–2310. https://doi.org/10.1152/AJPHEART.01029.2002/ASSET/IMAGES/LARGE/H40632336007.JPEG

Jama, H. A., Muralitharan, R. R., Xu, C., O'Donnell, J. A., Bertagnolli, M., Broughton, B. R. S., Head, G. A., & Marques, F. Z. (2022). Rodent models of hypertension. *British Journal of Pharmacology*, *179*(5), 918–937. https://doi.org/10.1111/bph.15650

Kang, N., Walther, T., Tian, X.-L., Bohlender, J., Fukamizu, A., Ganten, D., & Bader, M. (2002). Reduced hypertension-induced end-organ damage in mice lacking cardiac and renal angiotensinogen synthesis. *Journal of Molecular Medicine*, *80*(6), 359–366. https://doi.org/10.1007/s00109-002-0326-6

Kihara, M. (1998). Genetic deficiency of angiotensinogen produces an impaired urine concentrating ability in mice. *Kidney International*, *53*(3), 548–555. https://doi.org/10.1046/j.1523-1755.1998.00801.x

Krege, J. H., John, S. W. M., Langenbach, L. L., Hodgin, J. B., Hagaman, J. R., Bachman, E. S., Jennette, J. C., O'Brien, D. A., & Smithies, O. (1995). Male–female differences in fertility and blood pressure in ACE-deficient mice. *Nature*, *375*(6527), 146–148. https://doi.org/10.1038/375146a0

Kurtz, T. W., Griffin, K. A., Bidani, A. K., Davisson, R. L., & Hall, J. E. (2005). Recommendations for blood pressure measurement in humans and experimental animals. *Hypertension*, *45*(2), 299–310. https://doi.org/10.1161/01.HYP.0000150857.39919.cb

Laursen, J. B., Rajagopalan, S., Galis, Z., Tarpey, M., Freeman, B. A., & Harrison, D. G. (1997). Role of superoxide in angiotensin II-induced but not catecholamine- induced hypertension. *Circulation*, *95*(3), 588–593. https://doi.org/10.1161/01.CIR.95.3.588

Lázaro-Suárez, M. L., Gómez-Zamudio, J. H., Delgado-Buenrostro, N. L., Tanoue, A., Tsujimoto, G., & Villalobos-Molina, R. (2011). Angiotensin II modifies the expression of α1-adrenoceptors in aorta smooth muscle cells of α1D-adrenoceptor knockout mice. *Autonomic & Autacoid Pharmacology*, *31*(3–4), 57–63. https://doi.org/10.1111/j.1474-8673.2011.00467.x

Li, C., Wang, W., Kwon, T.-H., Knepper, M. A., Nielsen, S., Frøkiaer, J., & Frøkiaer Al-, J. (2003). Altered expression of major renal Na transporters in rats with bilateral ureteral obstruction and release of obstruction. *American Journal of Physiology-Renal Physiology*, *285*, 889–901. https://doi.org/10.1152/ajprenal.00170.2003.-Urinary

Lilley, E., Stanford, S. C., Kendall, D. E., Alexander, S. P. H., Cirino, G., Docherty, J. R., George, C. H., Insel, P. A., Izzo, A. A., Ji, Y., Panettieri, R. A., Sobey, C. G., Stefanska, B., Stephens, G., Teixeira, M., & Ahluwalia, A. (2020). ARRIVE 2.0 and the British Journal of Pharmacology: Updated guidance for 2020. *British Journal of Pharmacology*, *177*(16), 3611–3616. https://doi.org/10.1111/bph.15178

Livak, K. J., & Schmittgen, T. D. (2001). Analysis of relative gene expression data using real-time quantitative PCR and the $2-\Delta\Delta CT$ method. *Methods*, *25*(4), 402–408. https://doi.org/10.1006/meth.2001.1262

Lochard, N., Silversides, D. W., Van Kats, J. P., Mercure, C., & Reudelhuber, T. L. (2003). Brain-specific restoration of angiotensin II corrects renal defects seen in angiotensinogen-deficient mice. *Journal of Biological Chemistry*, *278*(4), 2184–2189. https://doi.org/10.1074/jbc.M209933200

Lohse, M. J., Engelhardt, S., & Eschenhagen, T. (2003). What is the role of β-adrenergic signaling in heart failure? *Circulation Research*, *93*(10), 896–906. https://doi.org/10.1161/01.RES.0000102042.83024.CA

Lopes, N. R., Milanez, M. I. O., Martins, B. S., Veiga, A. C., Ferreira, G. R., Gomes, G. N., Girardi, A. C., Carvalho, P. M., Nogueira, F. N., Campos, R. R., Bergamaschi, C. T., & Nishi, E. E. (2020). Afferent innervation of the ischemic kidney contributes to renal dysfunction in renovascular hypertensive rats. *Pflügers Archiv - European Journal of*

Physiology, *472*(3), 325–334. https://doi.org/10.1007/s00424-019-02346-4

Madsen, K., Marcussen, N., Pedersen, M., Kjærsgaard, G., Facemire, C., Coffman, T. M., & Jensen, B. L. (2010). Angiotensin II promotes development of the renal microcirculation through AT1 receptors. *Journal of the American Society of Nephrology*, *21*(3), 448–459. https://doi.org/10.1681/ASN.2009010045

Matsusaka, T., Nishimura, H., Utsunomiya, H., Kakuchi, J., Niimura, F., Inagami, T., Fogo, A., & Ichikawa, I. (1996). Chimeric mice carrying "regional" targeted deletion of the angiotensin type 1A receptor gene. Evidence against the role for local angiotensin in the in vivo feedback regulation of renin synthesis in juxtaglomerular cells. *Journal of Clinical Investigation*, *98*(8), 1867–1877. https://doi.org/10.1172/JCI118988

Moreira, N. J. D., dos Santos, F., Moreira, E. D., Farah, D., de Souza, L. E., da Silva, M. B., Moraes-Silva, I. C., Lincevicius, G. S., Caldini, E. G., & Irigoyen, M. C. C. (2020). Acute renal denervation normalizes aortic function and decreases blood pressure in spontaneously hypertensive rats. *Scientific Reports*, *10*(1), 21826. https://doi.org/10.1038/s41598-020-78674-8

Moreno, C., Hoffman, M., Stodola, T. J., Didier, D. N., Lazar, J., Geurts, A. M., North, P. E., Jacob, H. J., & Greene, A. S. (2011). Creation and characterization of a renin knockout rat. *Hypertension*, *57*(3), 614–619. https://doi.org/10.1161/HYPERTENSIONAHA.110.163840

Nagata, M., Tanimoto, K., Fukamizu, A., Kon, Y., Sugiyama, F., Yagami, K., Murakami, K., & Watanabe, T. (1996). Nephrogenesis and renovascular development in angiotensinogen-deficient mice. *Laboratory Investigation*, *75*(5), 745–753. http://www.ncbi.nlm.nih.gov/pubmed/8941219

Nakamori, H., Yoshida, S., Ishiguro, H., Suzuki, S., Yasuzaki, H., Hashimoto, T., Ishigami, T., Hirawa, N., Toya, Y., Umemura, S., & Tamura, K. (2018). Arterial wall hypertrophy is ameliorated by α2-adrenergic receptor antagonist or aliskiren in kidneys of angiotensinogen-knockout mice. *Clinical and Experimental Nephrology*, *22*(4), 773–781. https://doi.org/10.1007/s10157-017-1520-8

Neubauer, B., Schrankl, J., Steppan, D., Neubauer, K., Sequeira-Lopez, M. L., Pan, L., Gomez, R. A., Coffman, T. M., Gross, K. W., Kurtz, A., & Wagner, C. (2018). Angiotensin II short-loop feedback. *Hypertension*, *71*(6), 1075–1082. https://doi.org/10.1161/HYPERTENSIONAHA.117.10357

Niimura, F., Labosky, P. A., Kakuchi, J., Okubo, S., Yoshida, H., Oikawa, T., Ichiki, T., Naftilan, A. J., Fogo, A., Inagami, T., Hogan, B. L. M., & Ihikawa, I. (1995). Gene targeting in mice reveals a requirement for angiotensin in the development and maintenance of kidney morphology and growth factor regulation. *Journal of Clinical Investigation*, *96*(6), 2947–2954. https://doi.org/10.1172/JCI118366

Obayashi, K., Ando, Y., Terazaki, H., Yamashita, T., Nakamura, M., Suga, M., Uchino, M., & Ando, M. (2000). Mechanism of anemia associated with autonomic dysfunction in rats. *Autonomic Neuroscience*, *82*(3), 123–129. https://doi.org/10.1016/S0165-1838(00)00099-0

Okubo, S., Niimura, F., Matsusaka, T., Fogo, A., Hogan, B. L. M., & Ichikawa, I. (1998). Angiotensinogen gene null-mutant mice lack homeostatic regulation of glomerular filtration and tubular reabsorption. *Kidney International*, *53*(3), 617–625. https://doi.org/10.1046/j.1523-1755.1998.00788.x

Oliverio, M. I., Kim, H.-S., Ito, M., Le, T., Audoly, L., Best, C. F., Hiller, S., Kluckman, K., Maeda, N., Smithies, O., & Coffman, T. M. (1998). Reduced growth, abnormal kidney structure, and type 2 (AT2) angiotensin receptor-mediated blood pressure regulation in mice lacking both AT1A and AT1B receptors for angiotensin II. *Proceedings of the National Academy of Sciences*, *95*(26), 15496–15501. https://doi.org/10.1073/pnas.95.26.15496

Osborn, J. W., & Foss, J. D. (2017). Renal Nerves and Long-Term Control of Arterial Pressure. In *Comprehensive physiology* (pp. 263–320). Wiley. https://doi.org/10.1002/cphy.c150047

Osborn, J. W., Tyshynsky, R., & Vulchanova, L. (2021). Function of renal nerves in kidney physiology and pathophysiology. *Annual Review of Physiology*, *83*(1), 429–450. https://doi.org/10.1146/annurev-physiol-031620-091656

Pentz, E. S., Moyano, M. A., Thornhill, B. A., Sequeira Lopez, M. L. S., & Gomez, R. A. (2004). Ablation of renin-expressing juxtaglomerular cells results in a distinct kidney phenotype. *American Journal of Physiology-Regulatory, Integrative and Comparative Physiology*, *286*(3), R474–R483. https://doi.org/10.1152/ajpregu.00426.2003

Percie du Sert, N., Hurst, V., Ahluwalia, A., Alam, S., Avey, M. T., Baker, M., Browne, W. J., Clark, A., Cuthill, I. C., Dirnagl, U., Emerson, M., Garner, P., Holgate, S. T., Howells, D. W., Karp, N. A., Lazic, S. E., Lidster, K., MacCallum, C. J., Macleod, M., & Würbel, H. (2020). The ARRIVE guidelines 2.0: Updated guidelines for reporting animal research. *PLoS Biology*, *18*(7), e3000410. https://doi.org/10.1371/journal.pbio.3000410

Popova, E., Bader, M., & Krivokharchenko, A. (2005). Production of Transgenic Models in Hypertension. In *Hypertension* (Vol. 108) (pp. 33–50). Humana Press. 10.1385/1-59259-850-1:033

Porlier, G. A., Nadeau, R. A., Champlain, J., & Bichet, D. G. (1977). Increased circulating plasma catecholamines and plasma renin activity in dogs after chemical sympathectomy with 6-hydroxydopamine. *Canadian Journal of Physiology and Pharmacology*, *55*(3), 724–733. https://doi.org/10.1139/y77-097

Rabelo, L. A., Todiras, M., Nunes-Souza, V., Qadri, F., Szijártó, I. A., Gollasch, M., Penninger, J. M., Bader, M., Santos, R. A., & Alenina, N. (2016). Genetic deletion of ACE2 induces vascular dysfunction in C57BL/6 mice: Role of nitric oxide imbalance and oxidative stress. *PLoS ONE*, *11*(4), e0150255. https://doi.org/10.1371/journal.pone.0150255

Rodrigues, A. F., Todiras, M., Qadri, F., Campagnole-Santos, M. J., Alenina, N., & Bader, M. (2021). Increased angiotensin II formation in the brain modulates cardiovascular homeostasis and erythropoiesis. *Clinical Science*, *135*(11), 1353–1367. https://doi.org/10.1042/CS20210072

Rosendahl, A., Niemann, G., Lange, S., Ahadzadeh, E., Krebs, C., Contrepas, A., van Goor, H., Wiech, T., Bader, M., Schwake, M., Peters, J., Stahl, R., Nguyen, G., & Wenzel, U. O. (2014). Increased expression of (pro)renin receptor does not cause hypertension or cardiac and renal fibrosis in mice. *Laboratory Investigation*, *94*(8), 863–872. https://doi.org/10.1038/labinvest.2014.83

Schelling, P., Ganten, U., Sponer, G., Unger, T., & Ganten, D. (1980). Components of the renin-angiotensin system in the cerebrospinal fluid of rats and dogs with special consideration of the origin and the fate of angiotensin II. *Neuroendocrinology*, *31*(5), 297–308. https://doi.org/10.1159/000123092

Sequeira-Lopez, M. L. S., & Gomez, R. A. (2021). Renin cells, the kidney, and hypertension. *Circulation Research*, *128*(7), 887–907. https://doi.org/10.1161/CIRCRESAHA.121.318064

Sparks, M. A., Crowley, S. D., Gurley, S. B., Mirotsou, M., & Coffman, T. M. (2014). Classical Renin-Angiotensin System in Kidney Physiology. In *Comprehensive physiology* (Vol. 4) (pp. 1201–1228). Wiley. 10.1002/cphy.c130040.

Sugaya, T., Nishimatsu, S., Tanimoto, K., Takimoto, E., Yamagishi, T., Imamura, K., Goto, S., Imaizumi, K., Hisada, Y., Otsuka, A., Uchida, H., Sugiura, M., Fukuta, K., Fukamizu, A., & Murakami, K. (1995). Angiotensin II type 1a receptor-deficient mice with hypotension and Hyperreninemia. *Journal of Biological Chemistry*, *270*(32), 18719–18722. https://doi.org/10.1074/jbc.270.32.18719

Sun, Z., Cade, R., Zhang, Z., Alouidor, J., & Van, H. (2003). Angiotensinogen gene knockout delays and attenuates cold-induced hypertension. *Hypertension*, *41*(2), 322–327. https://doi.org/10.1161/01.HYP.0000050964.96018.FA

Takahashi, N., Lopez, M. L. S. S., Cowhig, J. E., Taylor, M. A., Hatada, T., Riggs, E., Lee, G., Gomez, R. A., Kim, H.-S., & Smithies, O. (2005). Ren1c homozygous null mice are hypotensive and Polyuric, but

heterozygotes are indistinguishable from wild-type. *Journal of the American Society of Nephrology*, *16*(1), 125–132. https://doi.org/10.1681/ASN.2004060490

Tamura, K., Umemura, S., Sumida, Y., Nyui, N., Kobayashi, S., Ishigami, T., Kihara, M., Sugaya, T., Fukamizu, A., Miyazaki, H., Murakami, K., & Ishii, M. (1998). Effect of genetic deficiency of angiotensinogen on the renin-angiotensin system. *Hypertension*, *32*(2), 223–227. https://doi.org/10.1161/01.HYP.32.2.223

Tanimoto, K., Sugiyama, F., Goto, Y., Ishida, J., Takimoto, E., Yagami, K. I., Fukamizu, A., & Murakami, K. (1994). Angiotensinogen-deficient mice with hypotension. *Journal of Biological Chemistry*, *269*(50), 31334–31337. http://www.jbc.org/content/269/50/31334.full.pdf, https://doi.org/10.1016/S0021-9258(18)31697-1

Todiras, M., Alenina, N., & Bader, M. (2017). Evaluation of Endothelial Dysfunction In Vivo. In *Methods in molecular biology* (Vol. 1527) (pp. 355–367). Springer. 10.1007/978-1-4939-6625-7_28

Tong, G.-X., Yu, W. M., Beaubier, N. T., Weeden, E. M., Hamele-Bena, D., Mansukhani, M. M., & O'Toole, K. M. (2009). Expression of PAX8 in normal and neoplastic renal tissues: An immunohistochemical study. *Modern Pathology*, *22*(9), 1218–1227. https://doi.org/10.1038/modpathol.2009.88

Tsuchida, S., Matsusaka, T., Chen, X., Okubo, S., Niimura, F., Nishimura, H., Fogo, A., Utsunomiya, H., Inagami, T., & Ichikawa, I. (1998). Murine double nullizygotes of the angiotensin type 1A and 1B receptor genes duplicate severe abnormal phenotypes of angiotensinogen nullizygotes. *Journal of Clinical Investigation*, *101*(4), 755–760. https://doi.org/10.1172/JCI1899

Vavřínová, A., Behuliak, M., Bencze, M., Vodička, M., Ergang, P., Vaněčková, I., & Zicha, J. (2019). Sympathectomy-induced blood pressure reduction in adult normotensive and hypertensive rats is counteracted by enhanced cardiovascular sensitivity to vasoconstrictors. *Hypertension Research*, *42*(12), 1872–1882. https://doi.org/10.1038/s41440-019-0319-2

Watanabe, H., Belyea, B. C., Paxton, R. L., Li, M., Dzamba, B. J., DeSimone, D. W., Gomez, R. A., & Sequeira-Lopez, M. L. S. (2021). Renin cell baroreceptor, a nuclear Mechanotransducer central for homeostasis. *Circulation Research*, *129*(2), 262–276. https://doi.org/10.1161/CIRCRESAHA.120.318711

Xiao, L., Kirabo, A., Wu, J., Saleh, M. A., Zhu, L., Wang, F., Takahashi, T., Loperena, R., Foss, J. D., Mernaugh, R. L., Chen, W., Roberts, J., Osborn, J. W., Itani, H. A., & Harrison, D. G. (2015). Renal denervation prevents immune cell activation and renal inflammation in angiotensin II–induced hypertension. *Circulation Research*, *117*(6), 547–557. https://doi.org/10.1161/CIRCRESAHA.115.306010

Xu, P., Costa-Goncalves, A. C., Todiras, M., Rabelo, L. A., Sampaio, W. O., Moura, M. M., Sousa Santos, S., Luft, F. C., Bader, M., Gross, V., Alenina, N., & Santos, R. A. S. (2008). Endothelial dysfunction and elevated blood pressure in mas gene-deleted mice. *Hypertension*, *51*(2), 574–580. https://doi.org/10.1161/HYPERTENSIONAHA.107.102764

Yanai, K., Saito, T., Kakinuma, Y., Kon, Y., Hirota, K., Taniguchi-Yanai, K., Nishijo, N., Shigematsu, Y., Horiguchi, H., Kasuya, Y., Sugiyama, F., Yagami, K., Murakami, K., & Fukamizu, A. (2000). Renin-dependent cardiovascular functions and renin-independent blood-brain barrier functions revealed by renin-deficient mice. *Journal of Biological Chemistry*, *275*(1), 5–8. https://doi.org/10.1074/jbc.275.1.5

Zhang, Y., Sun, Y., Ding, G., Huang, S., Zhang, A., & Jia, Z. (2015). Inhibition of mitochondrial Complex-1 prevents the downregulation of NKCC2 and ENaCα in obstructive kidney disease. *Scientific Reports*, *5*(1), 12480. https://doi.org/10.1038/srep12480

SUPPORTING INFORMATION

Additional supporting information can be found online in the Supporting Information section at the end of this article.

How to cite this article: Rodrigues, A. F., Todiras, M., Qadri, F., Alenina, N., & Bader, M. (2023). Angiotensin deficient FVB/N mice are normotensive. *British Journal of Pharmacology*, *180*(14), 1843–1861. https://doi.org/10.1111/bph.16051